ARMY RESEARCH LABORATORY

Progress in Modeling Pressure Oscillations in 30-mm Regenerative Liquid Propellant Guns (RLPGs)

by Terence P. Coffee

ARL-TR-1582 January 1998

The findings in this report are not to be construed as an official Department of the Army position unless so designated by other authorized documents.

Citation of manufacturer's or trade names does not constitute an official endorsement or approval of the use thereof.

Destroy this report when it is no longer needed. Do not return it to the originator.

Army Research Laboratory
Aberdeen Proving Ground, MD 21005-5066

ARL-TR-1582 **January 1998**

Progress in Modeling Pressure Oscillations in 30-mm Regenerative Liquid Propellant Guns (RLPGs)

Terence P. Coffee
Weapons and Materials Research Directorate, ARL

Abstract

Regenerative liquid propellant guns (RLPG) have been studied for many years. RLPG gun firings almost always show large high-frequency pressure oscillations. To study this phenomenon, a two-dimensional (2-D) axisymmetric fluid dynamics model of the combustion chamber/gun tube of an RLPG has been developed. High-frequency oscillations are generated naturally by the code. Recently, the code has been extended to three dimensions (3-D).

The results generally compare well with RLPG data; however, there are some recent cases that the code does not represent well. In this report, several extensions to the program are discussed in an attempt to improve the fidelity of the code. The most useful extension has been an intact-core model.

Acknowledgments

This work was supported in part by a grant of high-performance computing (HPC) time from the Department of Defense (DOD) HPC Center, U.S. Army Research Laboratory (ARL), Power Challenge Array.

The author would like to thank Ms. Gloria P. Wren and Mr. Joseph W. Colburn for their useful reviews of this manuscript.

INTENTIONALLY LEFT BLANK.

Table of Contents

INTENTIONALLY LEFT BLANK.

List of Figures

1. Introduction

A diagram of the U.S. Army Research Laboratory's (ARL) 30-mm concept VIC (6-C) regenerative liquid propellant gun (RLPG) is shown in Figure 1. The monopropellant in the liquid reservoir is prepressurized and located between the control piston and the injection piston. An external igniter injects hot gas into the combustion chamber. As the chamber is pressurized, the control piston is pushed to the left, opening the injection orifice. The motion of the control piston depends on the damper assembly. The injection piston follows the control piston, injecting the propellant from the reservoir through the annular orifice. The combustion takes place in the combustion chamber, and the gas then flows into the gun tube. There is a large area change from the chamber to the tube.

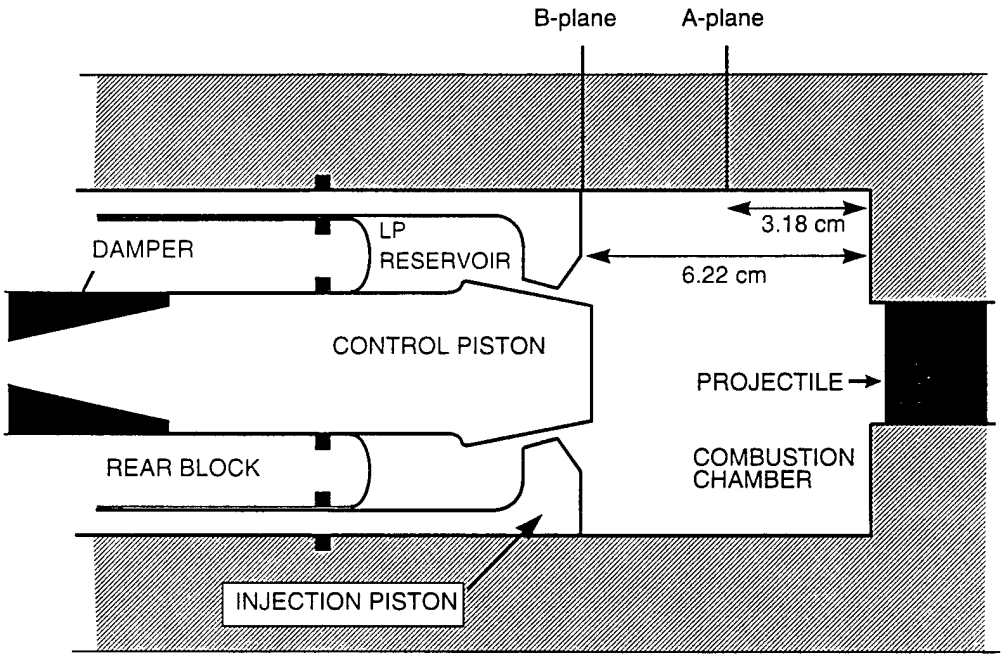

Figure 1. A Diagram of the ARL 30-mm Concept VIC RLPG.

Jet breakup and combustion are very complicated phenomena. Some of the injected liquid will be in an intact core. The length of this core depends, in part, on the gas density and the turbulence generated in the injector. Liquid will be stripped from the core by aerodynamic forces (primary breakup) and then further break up into droplets (secondary breakup). Due to the pressure and

temperature in the chamber, the drops heat and then combust. The gas generation rate depends on the local conditions. Almost all experimental work to measure quantities such as core length and droplet sizes has been for round jets at low pressures and low flow rates compared to the conditions in the RLPG. Due to the complexity of the phenomena and lack of information about annular jets at gun conditions, simplifying assumptions must be made in the numerical simulation.

Gun firings have been successfully simulated using a lumped parameter code RLPGUN (Coffee 1985, 1988; Coffee et al. 1991; Coffee and Wren 1996). The injected liquid is assumed to instantaneously break up into droplets and ignite. The droplet diameter is obtained from a theoretical formulation (Wolfe and Andersen 1964),

$$d = 5.1426\ v^{-4/3}\ D^{1/6}\ \sigma_L^{1/2}\ \mu_L^{1/3}\ \rho_L^{-1/6}\ \rho_G^{-2/3}\ ,$$

where d is the droplet diameter (cm), v is the relative velocity between the liquid and gas (cm/s), D is the diameter of the injector (cm), σ_L is the surface tension of the liquid (dynes/cm = g/s^2), μ_L is the liquid dynamic viscosity (poise = g/cm-s), ρ_L is the liquid density (g/cm^3), and ρ_G is the gas density (g/cm^3). The injection velocity is used as the relative velocity (assume gas in the chamber is stagnant). However, it has been found necessary to multiply the droplet diameter obtained by 30 to obtain the proper pressure rise rate. This has been hypothesized as due to coalescence in the very dense spray. Using this correlation, good agreement with data has been obtained for a wide variety of RLPG firings. Simulations have also been performed, assuming that most of the liquid is in an intact-core (Coffee et al. 1991). However, extrapolating standard intact-core models to gun conditions gives poor agreement with the experimental pressure-time data.

Essentially, all firings of RLPGs show large high-frequency pressure oscillations that cannot be modeled using a lumped parameter code. To consider spatial variations, a two-dimensional/three-dimensional (2-D/3-D) model LPOSC has been written for the combustion chamber and gun tube of an RLPG (Coffee 1992, 1994, 1995b). The model is not a complete gun code. The piston motions, liquid propellant injection rate, and injected droplet size are all obtained from a lumped

parameter code simulation. Due to lack of information about spray behavior under gun conditions, the very simple breakup model from the lumped parameter code has also been used in LPOSC.

Pressure waves are generated naturally by the model. As the liquid is injected, it starts to combust. Inertial confinement causes a small local pressure increase. This pressure wave leaves the neighborhood of the injector. The rate of gas generation at the injector decreases, due to the pressure dependence of the burn rate and the combustion of much of the propellant. The small pressure wave reflects from the walls and returns to the injector. Accumulated liquid now burns more rapidly, increasing the local pressure. After several iterations, the pressure waves become very large.

The experimental data suggest a limited regime for the jet breakup and combustion model. If the injected droplets are too large, the mean pressure rise is too slow. Experimental data indicate that the liquid burns very rapidly after being injected, and the mean pressure rise is primarily determined by the injection rate. On the other hand, if the injected droplets are too small, pressure oscillations will not be established. The liquid will burn rapidly with little dependence on the local pressure, and there is not enough liquid accumulation to enhance the pressure waves. Normally, LPOSC is implemented, assuming a minimum injected droplet diameter. Values from 50 μm to 200 μm can be used and still obtain the proper mean pressure rise and large oscillations. Best results are obtained with values between 100 μm and 150 μm.

In general, the model results are in reasonable agreement with experimental data from 30-mm and 155-mm guns. The model does show a simpler frequency structure than the data. In addition, there are some more complicated cases that the model does not represent well. One such case is flow dispersers (Coffee 1995a). Flow dispersers are extensions of the inner piston nose that are designed to more efficiently disperse and break up the liquid jet. The experimental data for guns fired with flow dispersers indicate a large reduction in pressure oscillations, while the model shows only a small effect.

Another issue is the proper value to use for the burn rate. All the shots considered in this report used the monopropellant XM46. The surface regression rate for a gelled XM46 propellant in a strand burner has been measured (McBratney 1980, 1981) as

$$1.64\ p^{0.103} \qquad 0 < p < 60\ .$$

McBratney observed some indication of a slope break in the burning rate above 60 MPa. Later work by Oberle and Wren (1991), based on closed-chamber tests on ungelled XM46 propellant, indicated a regression rate of

$$0.000577\ p^{2.009} \qquad 100 < p < 200\ .$$

In the code, a two-part burning rate is used, with the McBratney rate used under 67 MPa, and the Oberle and Wren rate used above 67 MPa.

More recently, the burning rate of MX46 was measured again for a gelled propellant in a strand burner with visual records of the surface (McBratney and Vanderhoff 1994). The data can be represented by the fit

$$1.64\ p^{0.103} \qquad 0 < p < 77$$

$$0.0139\ p^{1.2} \qquad 77 < p < 300\ .$$

The discrepancy in burning rates can partly be attributed to the different conditions. In the closed-chamber experiments, the propellant was placed inside a right circular cylinder within the closed chamber. To make the data analysis possible, the assumption was made that the surface regressed "cigarette fashion," and the exposed surface area was the area of the top of the cylinder. Experiments at lower pressures indicate that the surface was uneven. It was felt that, at the higher pressures, the surface would be less disturbed, and this assumption was used in the analysis. The

closed-chamber burning rate is probably an upper limit on the burning rate, since any disturbance of the surface would give a larger surface area and, hence, a greater apparent burning rate.

In the strand-burner experiments, a gelling agent was added to the propellant to ensure that the surface area was undisturbed. However, the addition of the gelling agent may decelerate the burning rate (Klein 1992). The actual high-pressure regression rate is expected to be between the two measured rates, but closer to the strand-burner rate.

The model has normally been implemented with the closed-chamber rate. When the strand-burner rate is used instead, the oscillations are much too small compared to experimental data. It would be more satisfying to use the more accurate strand-burner rate to obtain good agreement with the experimental data.

This report discusses several new options added to the model to examine the discrepancy between experiment and simulation for some of the firings. As discussed previously, the jet breakup and combustion cannot be modeled in complete detail. The procedure has been to add physical effects that are expected to still be important at gun conditions and to study the effects in the model.

2. Piston Motion

In the original model, the relative motion of the pistons was ignored in order to simplify the regriding process. The grid has previously been initialized with the pistons at their maximum separation for a given experiment, and the pistons are moved back as a unit. The code has now been generalized to allow the pistons to move independently. Initially, the pistons have a small gap between them (Figure 2). As the pistons separate, the grid points on the injection piston (outer piston) move as a unit at the injection piston velocity. The axial velocity of the points on the control piston (inner piston) vary between the control piston velocity at the right and the injection piston velocity at the left. The radial velocity is chosen so that the points move along the surface of the piston. Points on the outer wall above the control piston are uniformly compressed. Points to the

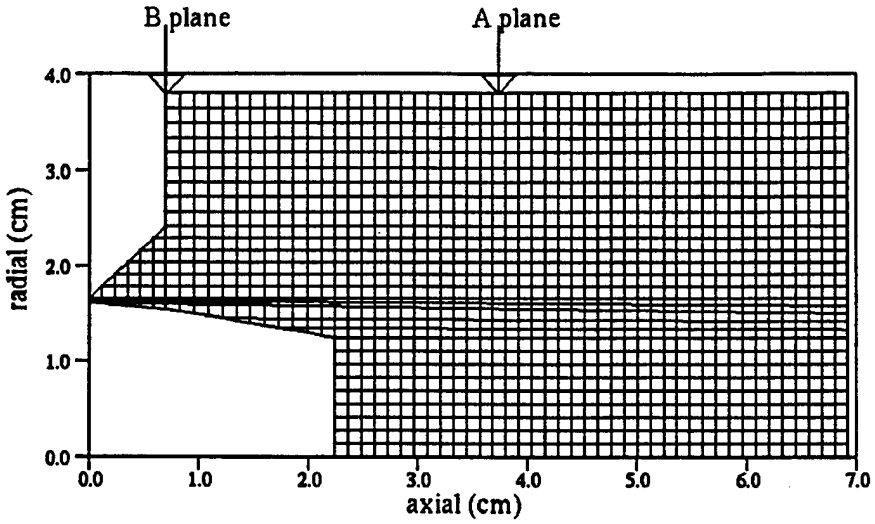

(a) Initial Grid.

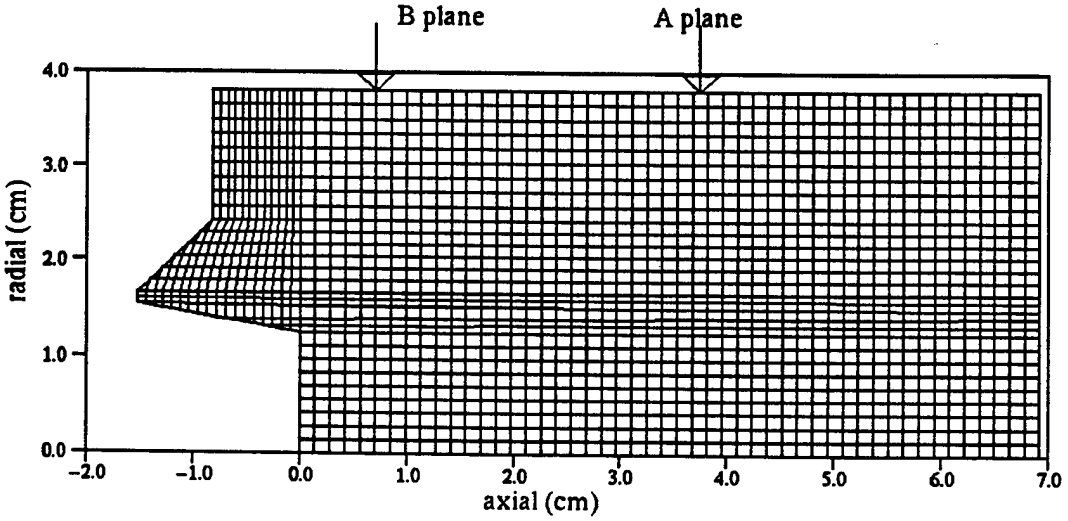

(b) Grid Near Maximum Piston Separation.

Figure 2. Grid for a 30-mm Small-Charge Gun Firing, Round 161.

right of the control piston are stretched uniformly, and new grid points are added as necessary. Points under the chambrage (if any) are not moved. This improvement to the model had only a small effect on the previous results.

3. Drag

For the 2-D model, the grid divides the combustion chamber into annular control volumes. The scalar quantities (pressure, temperature, and density) are assumed to be uniform within a control volume. The axial and radial velocities are defined on the vertices of the control volumes. The position of the vertices may be arbitrarily specified as a function of time. A two-phase formulation is used. Each control volume may have liquid, gas, or both, where the pressure in the liquid and gas phases is assumed to be the same. The liquid and gas have different densities. Previously, it has been assumed that the liquid and gas have the same velocity at any given point (infinite drag). A version of the code has been written without this assumption.

There are now separate momentum equations for the liquid and gas. The pressure gradient acts on the gas and liquid proportionally to the volume fraction. That is, let ϵ be the volume fraction in a region (volume of gas over total volume), and let A_x be the axial cross-sectional area of the region. The force exerted on the fluid is proportional to the axial pressure gradient times the area. The total force is multiplied by ϵ to obtain the axial force on the gas, and by $1 - \epsilon$ to obtain the force on the liquid. The radial force is obtained in the same manner.

The drag correlation used was developed by Gough (1983) for particles and shows good agreement with experimental data (Fox and McDonald 1985). The liquid is assumed to be in the form of spherical droplets. Distortion of the drops by the gas flow is ignored. Then the Reynolds number is

$$Re = \rho_G \, \text{abs} \left(u_G - u_L\right) d/\mu_G \, ,$$

where ρ_G is the gas density (g/cm^3), u_G is the gas velocity (cm/s), u_L is the liquid velocity (cm/s), d is the droplet diameter (cm), and μ_G is the gas dynamic viscosity (poise = g/cm-s). The drag coefficient is then

$$C_D = 2.5\ Re^{-0.081}\ .$$

The drag force is given by the formula

$$\text{drag} = C_D\ (1 - \epsilon)\ \rho_G\ \text{abs}\left(u_G - u_L\right)\left(u_G - u_L\right) V/d\ ,$$

where ϵ is the gas-volume fraction (porosity) in the control volume V. This formula has units of dynes = g-cm/s^2.

When a 30-mm gun was simulated with no model modifications except the separate momentum equations and the drag law, the new version of the code showed no oscillations at all. A 155-mm gun simulation still showed oscillations, starting a few milliseconds later than previous model results. The source of the discrepancy was eventually discovered. As previously mentioned, the first step in generating pressure oscillations is to obtain a small local pressure rise from combustion and inertial confinement. The generated gas has a much lower density than the liquid. In the new formulation, the pressure preferentially accelerates the gas. The gas is moved rapidly away from the liquid, and it is more difficult to generate an initial pressure rise.

The aforementioned analysis suggests that the two versions of the code (with and without separate gas and liquid-momentum equations) should approach the same answer as the droplet size is decreased, since for small enough drops, the liquid quickly comes into equilibrium with the gas. This turns out to be the case. However, the droplets have to be so small that oscillations are not generated.

The other consideration is the natural frequencies of the system. In 30-mm gun experiments, the most common frequencies seen are near 17 kHz (first radial mode of the chamber) and 24 kHz (first radial mode for the annular region between the control piston and the chamber). The local velocities then also change rapidly, and the liquid and gas cannot easily equilibrate. In the 155-mm guns, the most common frequency is 6 kHz (first radial mode for the annulus). With the lower frequency, there is more time for the liquid and gas to equilibrate, and oscillations are eventually generated.

4. Droplet Distribution

Previously, it has been assumed that the droplets in any given control volume are all the same size. This is assumed to be the Sauter-mean diameter, the diameter that preserves the surface area of the original distribution. In the version of the code with infinite drag, this is probably a good approximation. However, the code upgrades allow the gas and liquid to have different velocities. Smaller droplets will tend to move with the gas, while larger droplets will tend to move with the injected trajectory. Different droplet sizes will cause more dispersion of the liquid, possibly creating more complicated oscillations. A droplet distribution model was implemented to study these effects.

Experimental data (Simmons 1977) indicate that both the primary and the secondary breakup can be correlated assuming a root-normal distribution (the square root of the droplet diameters fall on a normal distribution). The mass-median diameter (half the mass is in droplets with a smaller diameter) is 1.2 times the Sauter-mean diameter. There is evidence that this holds even for dense sprays (Faeth, Hsiang, and Wu 1995). This correlation was extrapolated to gun conditions.

Consider a distribution of drops in a control volume. Define a probability distribution $M_L(r)$ = mass of drops with radius between r and r + dr. Let m(r) be the rate of consumption of drops with radius r, or

$$m(r) = M_L(r)\ (3/r)\ ap^n,$$

where ap^n is the surface regression rate. From the definition of $M_L(r)$,

$$\partial M_L(r)/\partial t = -m(r) - \partial M_L(r)/\partial r\ \ \partial r/\partial t\ .$$

That is, the rate at which the mass of drops with radius r changes is the loss due to combustion into gas plus the gain/loss as drops burn down to a smaller size.

The distribution is discretized to change the partial differential equation into a set of ordinary differential equations. Assume we break the distribution up into N groups or bins. The drops in bin k are assumed to have an average droplet diameter $dav(k)$. Then

$$m(k) = M_L(k) \left(6/dav(k)\right) ap^n$$

is the mass burning rate for each class, and the total mass burning rate is

$$m = \Sigma\, m(k) .$$

To derive the governing differential equations, assume that in any bin, the mass is evenly distributed among the possible diameters. Let $d_{inc}(k) = db(k+1) - db(k)$ be the diameter difference between the largest and smallest droplets in a group. Then over a time step Δt,

$$\Delta M_L(k) = -m(k)\Delta t + M_L(k)\ \Delta d/d_{inc}(k) - M_L(k+1)\ \Delta d/d_{inc}(k+1) .$$

That is, the rate of change of the mass in group k is the loss through combustion, the loss as drops become smaller than the class limit, and the gain as drops from the next-largest class become small enough to fit into class k. The quantity Δd is the change in diameter of the droplets (always a negative number due to combustion). In a control volume, the burning rate is the same for all drops, so the diameter of all the drops changes by the same amount. That is,

$$\Delta d = -2\ ap^n$$

or twice the linear regression rate. Then taking the limit as Δt goes to zero, we obtain a set of N ordinary differential equations

$$dM_L(k)/dt = -m(k) + \left[-M_L(k)/d_{inc}(k) + M_L(k+1)/d_{inc}(k+1)\right] 2ap^n .$$

Of course, for class one, there is no loss term to a smaller class, and, for the largest class, there is no gain term from a larger class.

For the runs reported here, there are 10 droplet classes. The boundaries of the droplet classes are chosen so the square root of the boundary droplet diameters are equally spaced. Given the Sauter-mean diameter of the injected liquid, it is then broken up, assuming the root-normal distribution. The code must now track the mass in each class in each control volume, as well as the velocities of each class.

In looking at simplified test problems, it was found that a root-normal distribution of droplets burns more slowly than a monosized distribution with the same Sauter-mean diameter. By definition, they start combusting the same, since they have the same surface area. However, for the root-normal distribution, the small droplets burn out rapidly, leading to a large reduction in the surface area. The large droplets take longer to decrease in size. So the Sauter-mean diameter does not capture all the behavior of a distribution.

This was added to the updated code, with separate momentum equations for the liquid and gas. For gun simulations, there were no significant differences from the monosized droplet distribution. For the 30-mm gun, there were still no significant oscillations. For the 155-mm gun, the oscillations still started later and were somewhat smaller than for the previous version of the code.

5. Heat Transfer and Ignition Delay

Previously, it was assumed that the liquid burned immediately upon being injected into the chamber. In practice, the liquid must first be heated. Ignoring radiation, heat transfer from a hot gas to a liquid droplet is given by

$$M_d \, c_{p,d} \, dT_d/dt = h \, S \, (T_g - T_d) \, ,$$

where M_d is the mass of the droplet (g), $c_{p,d}$ is the specific heat at constant pressure (J/g-K), h is the heat transfer coefficient (J/cm^2-K-s), S is the surface area (cm^2), T_g is the gas temperature (K), and T_d is the droplet temperature. The heat-transfer coefficient may be given by (Ranz and Marshall 1952)

$$h = k_g(2 + 0.6\ Re_d^{1/2}\ Pr^{1/2})/d_d ,$$

where k_g is the thermal conductivity of the gas (J/cm-K-s), Re_d is the Reynolds number of the droplet, Pr is the Prandtl number, and d_d is the diameter of the droplet. This correlation implies that the heat transfer goes up dramatically when the gas is moving relative to the drop. The Reynolds number for the drop is

$$Re_d = \rho_g\ u\ d/\mu_g$$

where ρ_g is the gas density (g/cm^3), u is the relative velocity between the gas and liquid (cm/s), and μ_g is the kinematic viscosity of the gas (poise = g/cm-s). The Prandtl number is

$$Pr = c_{p,g}\ \mu_g/k_g ,$$

where $c_{p,g}$ is the specific heat at constant pressure for the gas (J/g-K). The droplets are assumed to heat uniformly.

This was implemented in the code. Combustion was turned off until the droplets reached an ignition temperature. Experiments at atmospheric pressure indicate that the propellant starts to react slowly around 400 K (Klein, Leveritt, and Baer 1991). In the model, the droplets heat uniformly. In practice, there will be a temperature gradient, and the surface will be hotter than the interior. On the other hand, the liquid may have to be heated past the ignition temperature to combust rapidly.

With this addition to the model described previously, large pressure oscillations can be generated. Given a root-normal distribution, the smaller droplets will tend to move with the gas, and there is enough liquid accumulation so that pressure oscillations can build and intensify.

6. 30-mm Gun

Round 161, a small-charge (91 cm^3) firing in the 30-mm gun (Colburn et al. 1995) was modeled. Several pressure ports are located in the A plane (near the tube) and in the B plane (nearer the pistons). Most ports are standard-recessed, grease-packed, two-diameter ports. The A90 (90° from top of gun) and B30 (30° from top of gun) gauge locations are flush-mounted ports, which are expected to record oscillations more accurately (Rosenberger 1994). However, the flush-mounted ports record the mean pressure lower than the actual pressure, due to thermal drift of the exposed gauges. For this shot, there was also a flush-mounted pressure gauge in the face of the control piston.

The shot was first modeled using the standard assumptions (liquid instantaneously breaks up into droplets and begins burning). A minimum droplet diameter of 200 μm was assumed. The pistons were allowed to move separately. The experimental pressure at the B30 gauge is compared with the 2-D simulation in Figure 3. The results at the A plane were similar. This shot was one of a small number where the pressure was also recorded on the face of the control piston. The pressure gauge breaks down just before 7 ms (Figure 4). The model produces oscillations that are roughly correct in magnitude.

Figures 5–7 compare the Fourier transforms of the data and the model. The data primarily show a 19-kHz signal (first radial for the chamber). The model shows reasonable agreement with this frequency at the B plane. The relatively large 200-μm-diameter droplet must be assumed in the model to obtain the proper frequency. The combustion is pushed toward the end of the piston. If a smaller droplet size is assumed, most of the combustion occurs over the control piston, and a frequency near 23-kHz is generated (first radial mode for an annulus). Agreement is also reasonable at the A plane, although the model does show the 23-kHz signal. However, the 19-kHz frequency

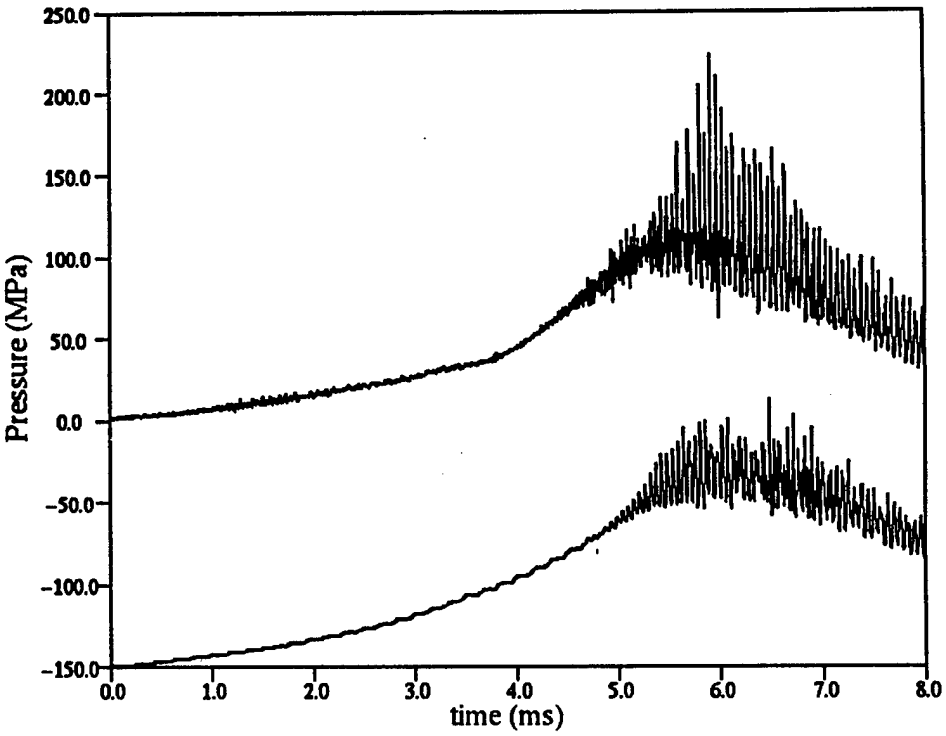

Figure 3. 30-mm Gun, Round 161. B30 Gauge (Top). Standard Simulation, 200-µm-Droplet Diameter (Bottom).

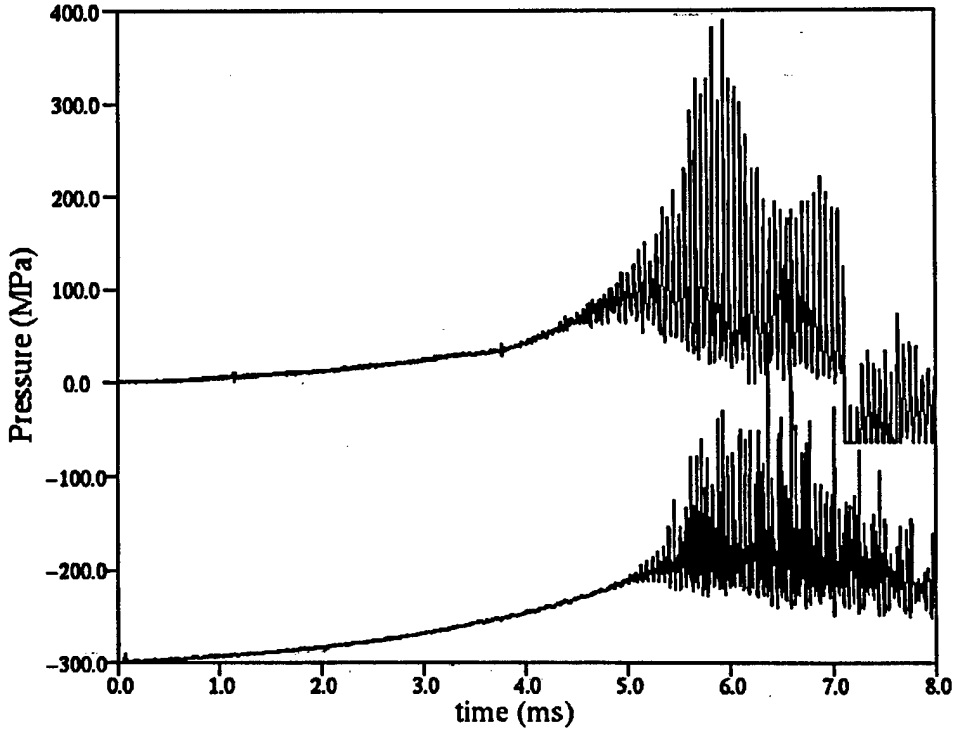

Figure 4. 30-mm Gun, Round 161. Control Piston Gauge (Top). Standard Simulation, 200-µm-Droplet Diameter (Bottom).

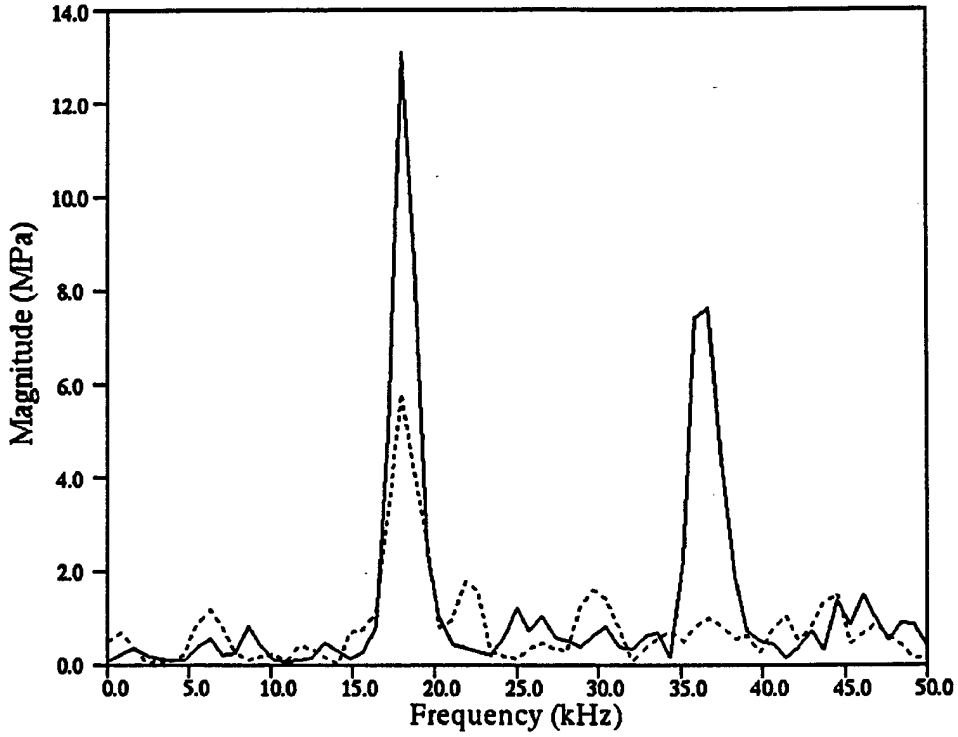

Figure 5. 30-mm Gun, Round 161. FFT, 5.5–6.5 ms. B30 Gauge (Line). Standard Simulation, 200-µm-Droplet Diameter (Dot).

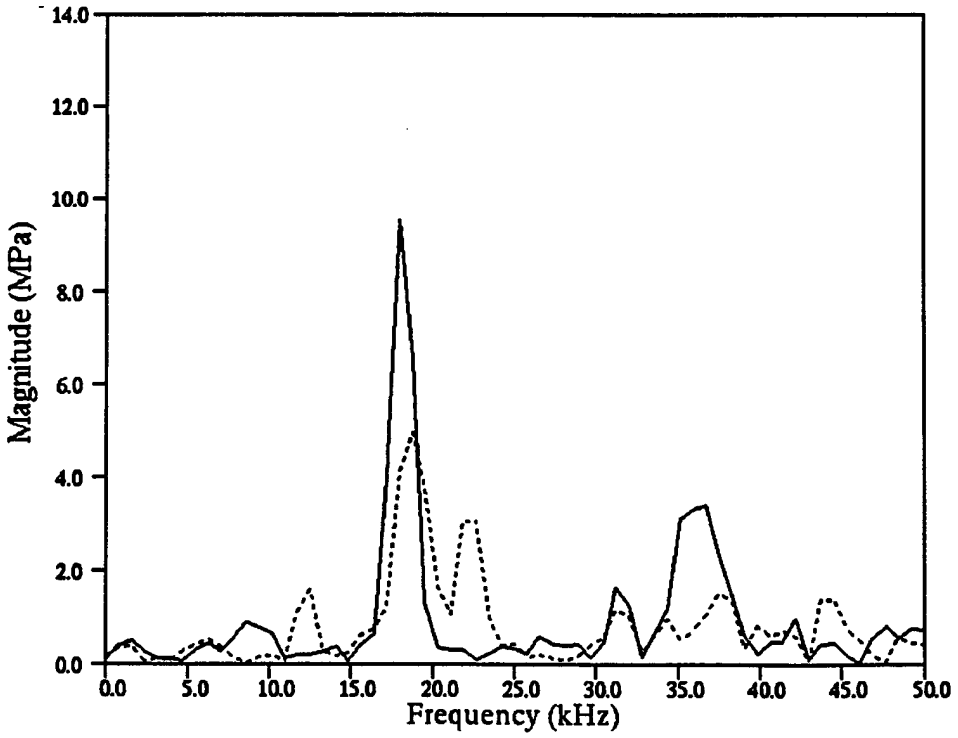

Figure 6. 30-mm Gun, Round 161. FFT, 5.5–6.5 ms. A90 Gauge (Line). Standard Simulation, 200-µm-Droplet Diameter (Dot).

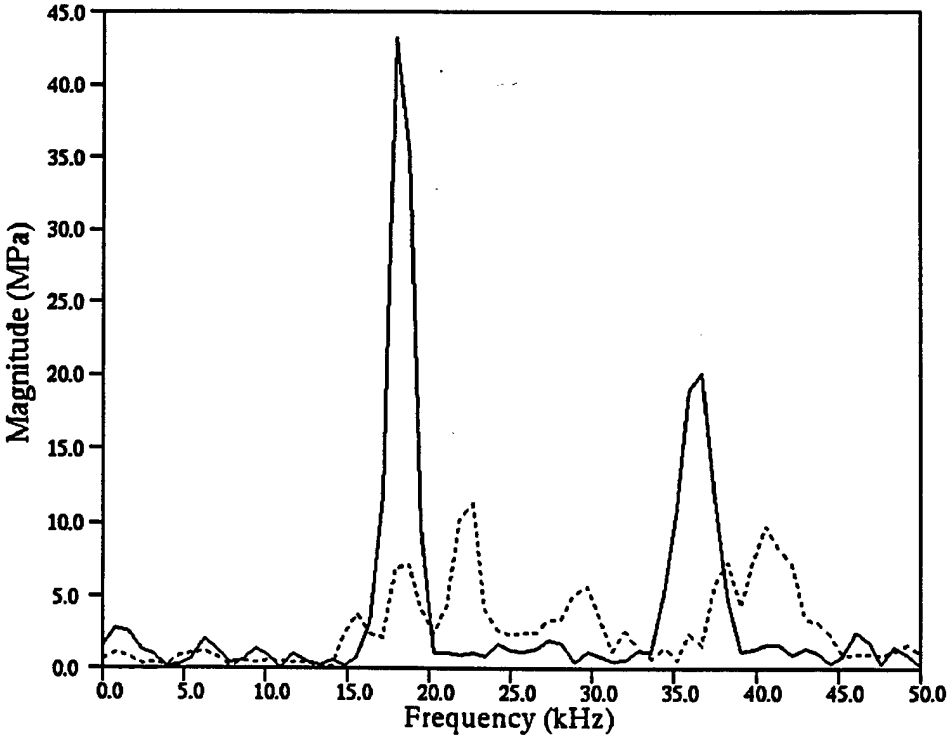

Figure 7. 30-mm Gun, Round 161. FFT, 5.5–6.5 ms. Control Piston Gauge (Line). Standard Simulation, 200-μm-Droplet Diameter (Dot).

does not turn up in the model at the center line on the control piston. The mode generated by the model is not a standard first-radial mode. Much of the combustion is still above the control piston, and pressure waves moving along the control piston interfere with the radial pressure waves. The highest pressure oscillations are near the injector.

The poor comparison between experiment and the model results, particularly at the control piston gauge, motivated work on the combustion model. Apparently, the combustion zone must be pushed toward the gun tube to generate a purely radial mode for the cyliner.

The modified model was then run, but without a droplet distribution. The droplet diameter at a point was represented by a single number, the Sauter-mean diameter. There were separate momentum equations for the gas and the liquid. The ignition temperature was set to 350 K. The mean-injected droplet size was found by multiplying the Wolfe and Anderson correlation by five, with a minimum-injected droplet diameter of 25 μm.

The results at the B plane are shown in Figure 8. The oscillations start too soon and are somewhat too large. The Fourier transforms are shown in Figures 9 and 10. The model shows a clean 23-kHz signal (first radial for the annulus). This signal is also large at the center line. A number of other parameters were tried, but it proved impossible to excite the 19-kHz signal and still obtain a reasonable mean-pressure rise.

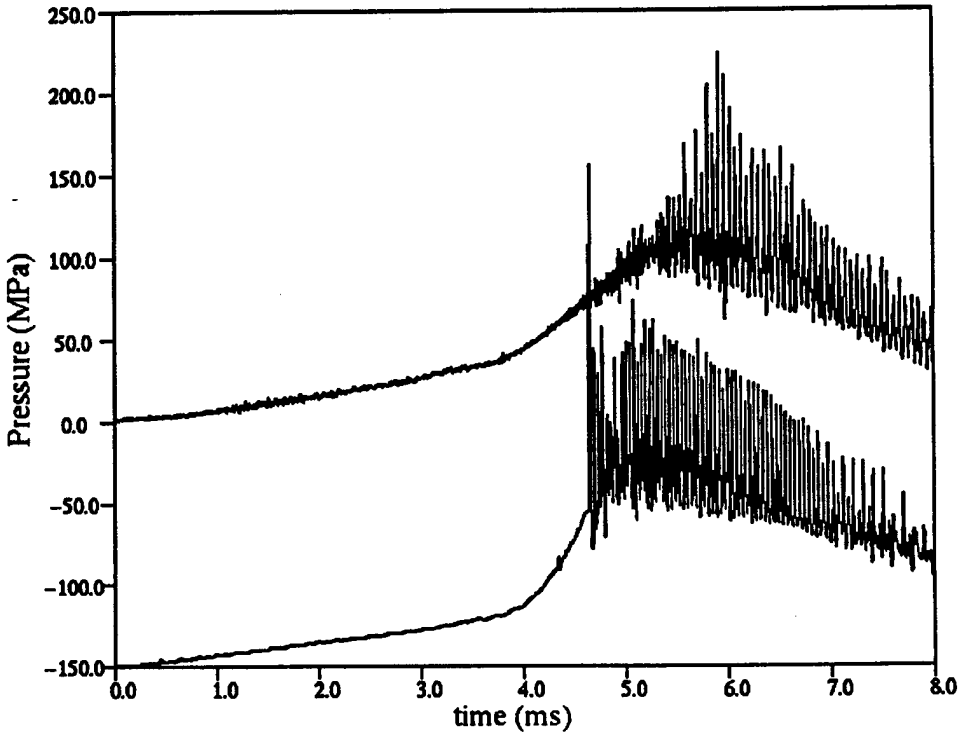

Figure 8. 30-mm Gun, Round 161. B30 Gauge (Top). Simulation, Separate Momentum Equations (Bottom).

Finally, the modified model was run with a droplet distribution. Injected droplets were assumed to be between 5 and 500 μm in diameter. The droplet distribution was approximated by 10 bins. The ignition temperature was set to 350 K. The mean-injected droplet size was found by multiplying the Wolfe and Anderson correlation by 10, with a minimum-injected droplet diameter of 25 μm.

The oscillations now start later and are not quite as large (Figure 11). The model excites primarily the 24-kHz mode (Figures 12 and 13). The droplet distribution does not lead to a more complicated spectrum.

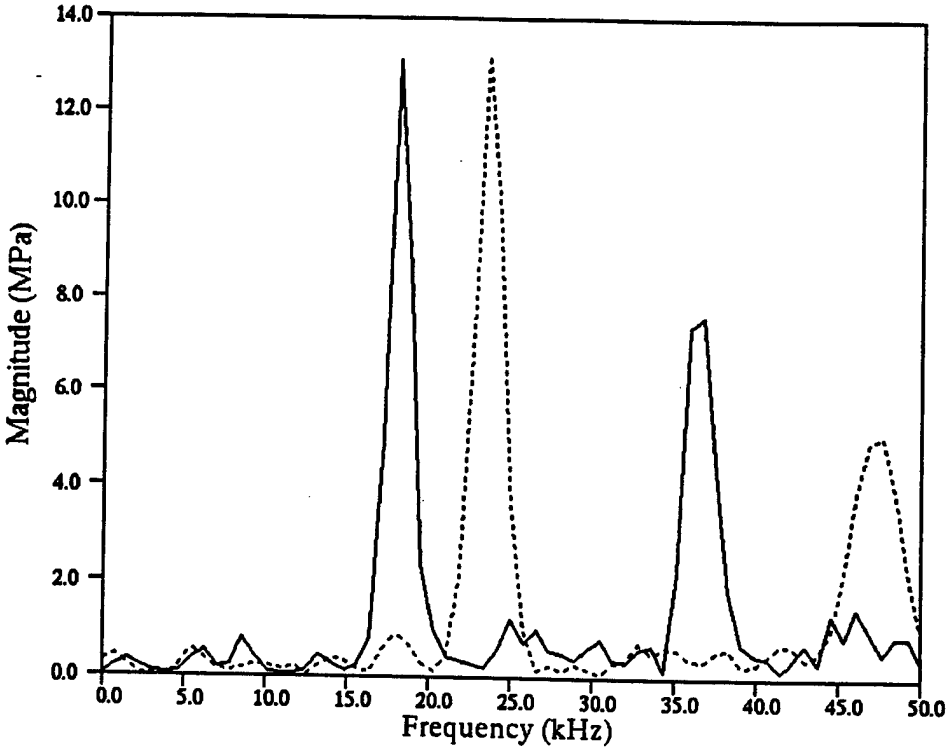

Figure 9. 30-mm Gun, Round 161. FFT, 5.5–6.5 ms. B30 Gauge (Line). Simulation, Separate Momentum Equations (Dot).

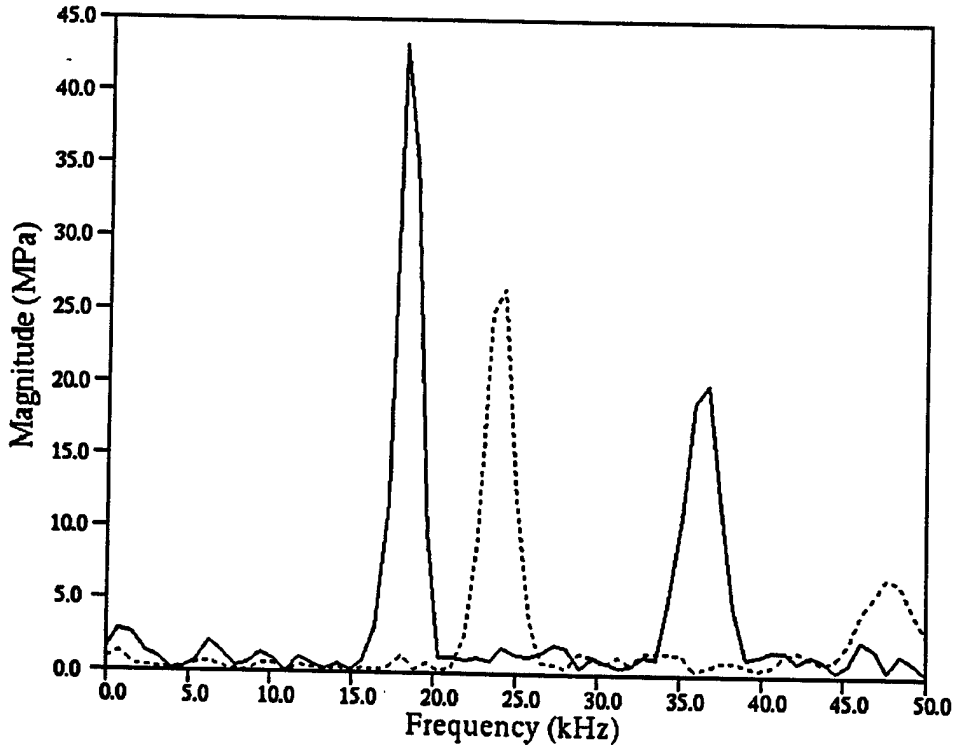

Figure 10. 30-mm Gun, Round 161. FFT, 5.5–6.5 ms. Control Piston Gauge (Line). Simulation, Separate Momentum Equations (Dot).

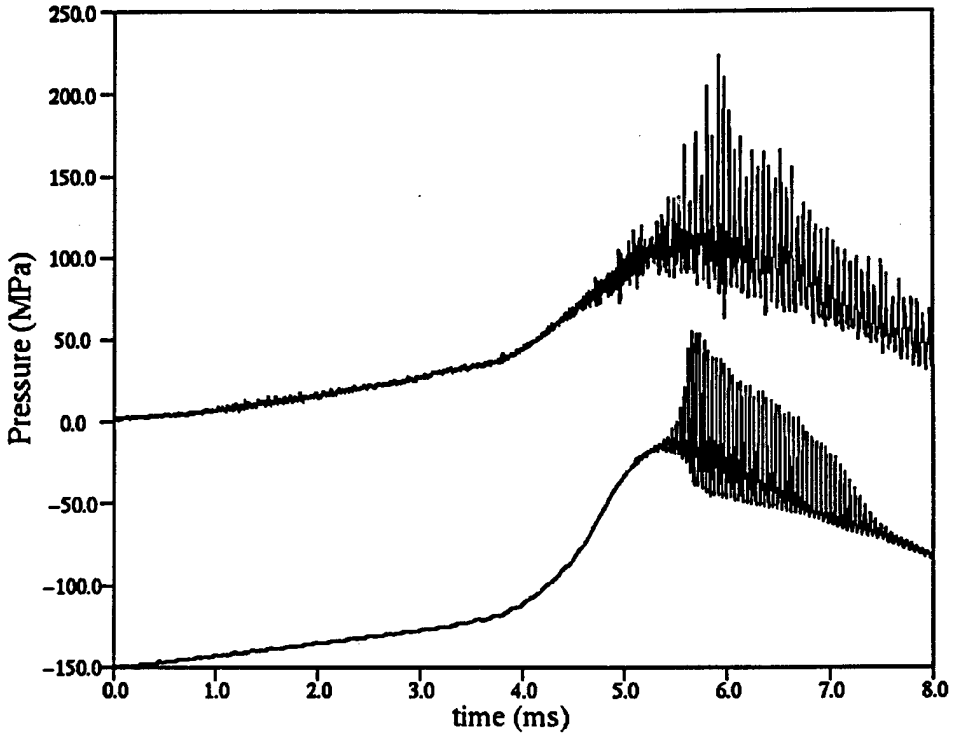

Figure 11. 30-mm Gun, Round 161. B30 Gauge (Top). Simulation, Droplet Distribution (Bottom).

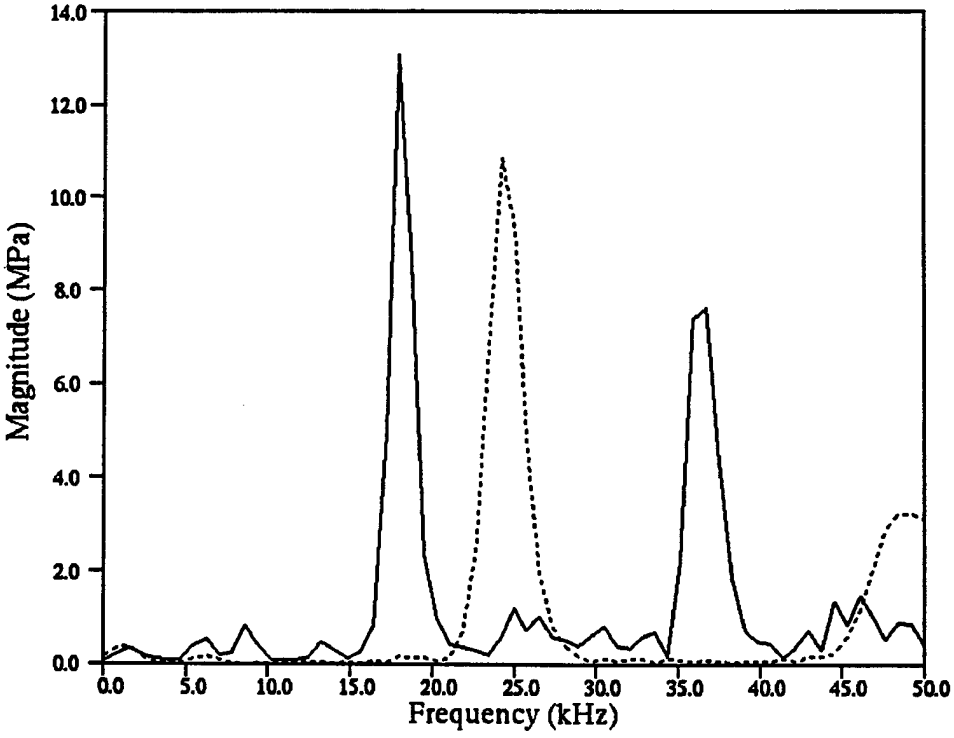

Figure 12. 30-mm Gun, Round 161. FFT, 5.5–6.5 ms. B30 Gauage (Line). Simulation, Droplet Distribution (Dot).

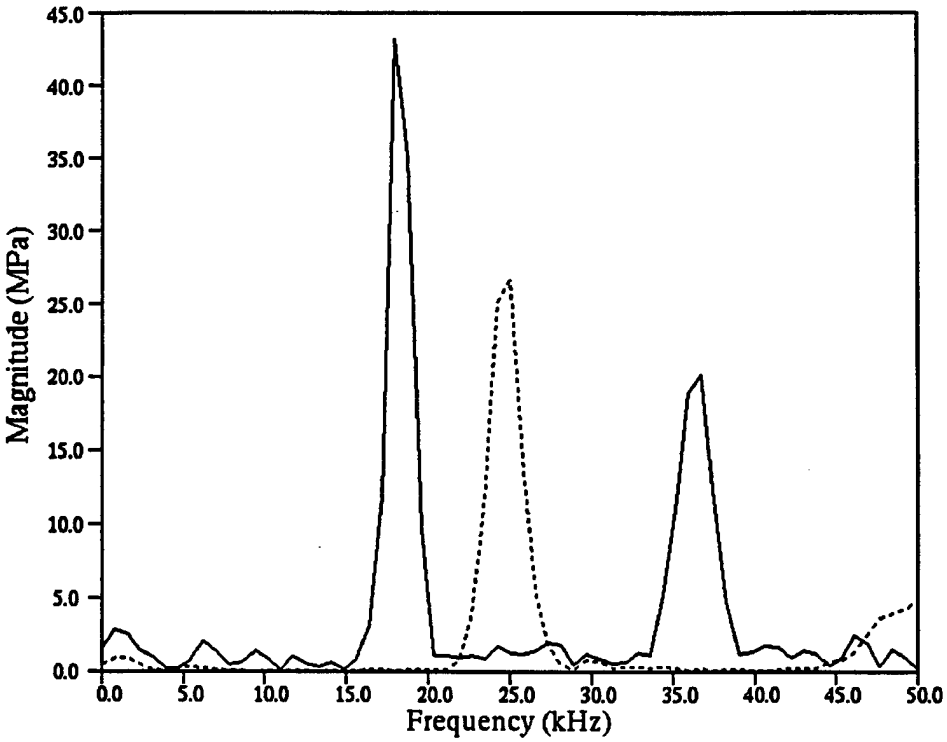

Figure 13. 30-mm Gun, Round 161. FFT, 5.5–6.5 ms. Control Piston Gauge (Line). Simulation, Droplet Distribution (Dot).

The results using the modified code do not show an improvement over the standard code in representing experimental data, and the code takes at least an order of magnitude longer to run. Additional physics associated with jet breakup appear to be needed.

7. Intact Core

The aforementioned work indicates that combustion is delayed in some cases until liquid is near the end of the control piston. While this can be accomplished in the model by assuming large droplets, the agreement between model and experiment at the center line of the gun is very poor. Also, simulations performed using separate momentum equations for the liquid and gas indicate that pressure oscillations can only be generated if the droplets are relatively small. Another mechanism to delay combustion appears to be present.

It is known that at least some of the liquid will be an intact-core rather than in the form of droplets. Intact-core models were examined in the context of the lumped parameter code and found to not be satisfactory (Coffee et al. 1991). However, based on the poor comparisons between model and experiment shown previously using droplet models, intact-core models were reexamined.

The length of a jet intact core for a circular pressure atomized jet can be approximated by

$$L/d = C\left(\rho_L/\rho_G\right),$$

where L is the length of the intact core, d is the diameter of the orifice, ρ_L is the liquid density, ρ_G is the gas density, and C is a constant between 7 and 16 (Faeth, Hsiang, and Wu 1995). Almost all work on jet breakup has been performed for $\rho_L/\rho_G > 500$. In the gun, this ratio is close to 10 near peak pressures.

This formula was implemented in the code, where ρ_L is the density of the injected liquid, ρ_G is the average gas density in the combustion chamber, and d is the hydraulic diameter of the annulus. It is desirable to use the simpler version of the code, where the gas and the liquid have the same velocity at any given point, since the run times are much shorter. The incoming liquid is assumed to break up into droplets using the Wolfe and Andersen correlation, but without a multiplying factor. A minimum droplet size of 10 μm is used. To model the core, combustion is set to zero. When liquid leaves the core, it is assumed to instantaneously break up into droplets and begin burning. The gas and liquid velocities instantaneously equilibrate. For the small droplets now used, these are reasonable assumptions. The model is now simple enough to be tractable.

At first, the intact core was assumed to be directly in front of the injector. It proved impossible to obtain satisfactory results. However, an alternate approach was tried based on recent experimental data (Birk, McQuaid, and Gross 1995). In the experiment, liquid propellant was injected through an annulus into relatively high-pressure gas, and the core was studied using flash x-rays. The core very quickly collapsed toward the center line.

Based on these results, the core was assumed to extend radially from the top of the injector to the top of the control piston. The area under the injector may not entirely be an intact core, but may also include a dense spray region. The assumption is that hot gas cannot get under the core and above the control piston and ignite the spray. The value of the constant is chosen to obtain approximately the correct mean pressure rise.

This version of the code was run for round 161. The constant C was set equal to 3.0. The results at the B plane are shown in Figure 14. The oscillations are somewhat low in magnitude. However, the magnitude of the oscillations at the center line from the model compares favorably to the data (Figure 15).

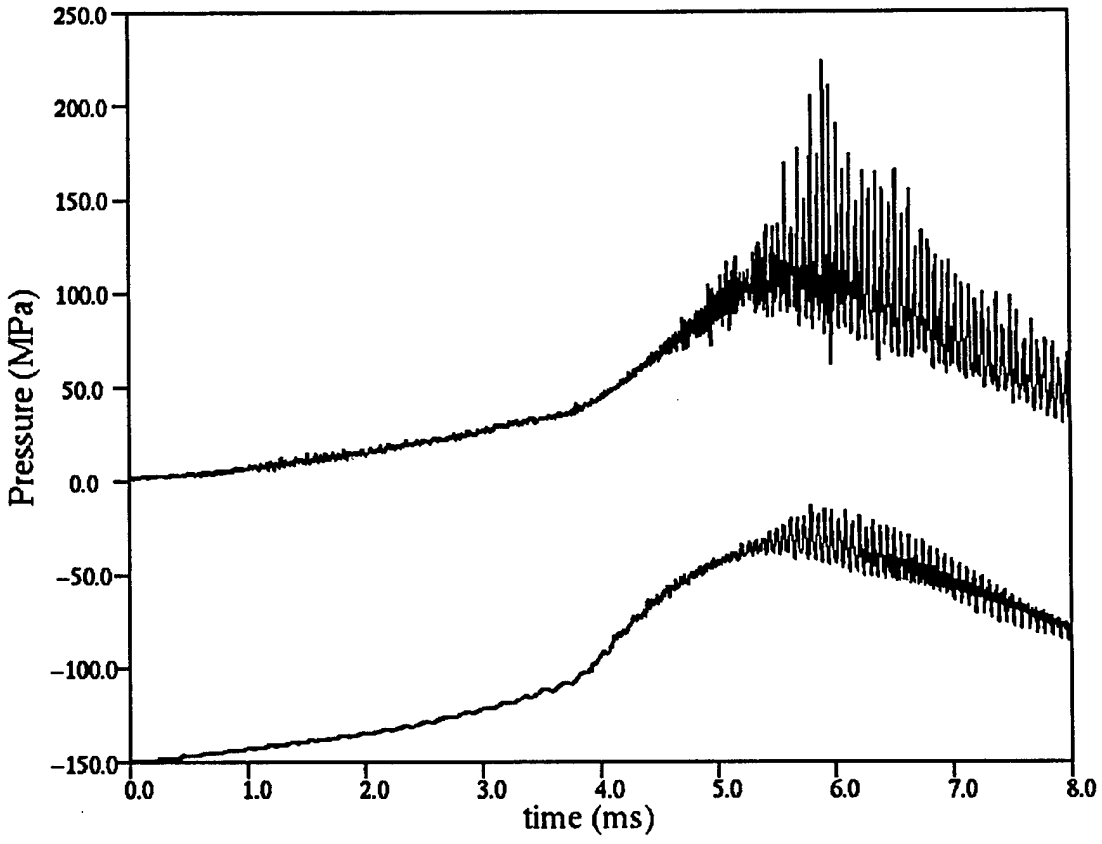

Figure 14. 30-mm Gun, Round 161. B30 Gauge (Top). Intact-Core Model, C = 3 (Bottom).

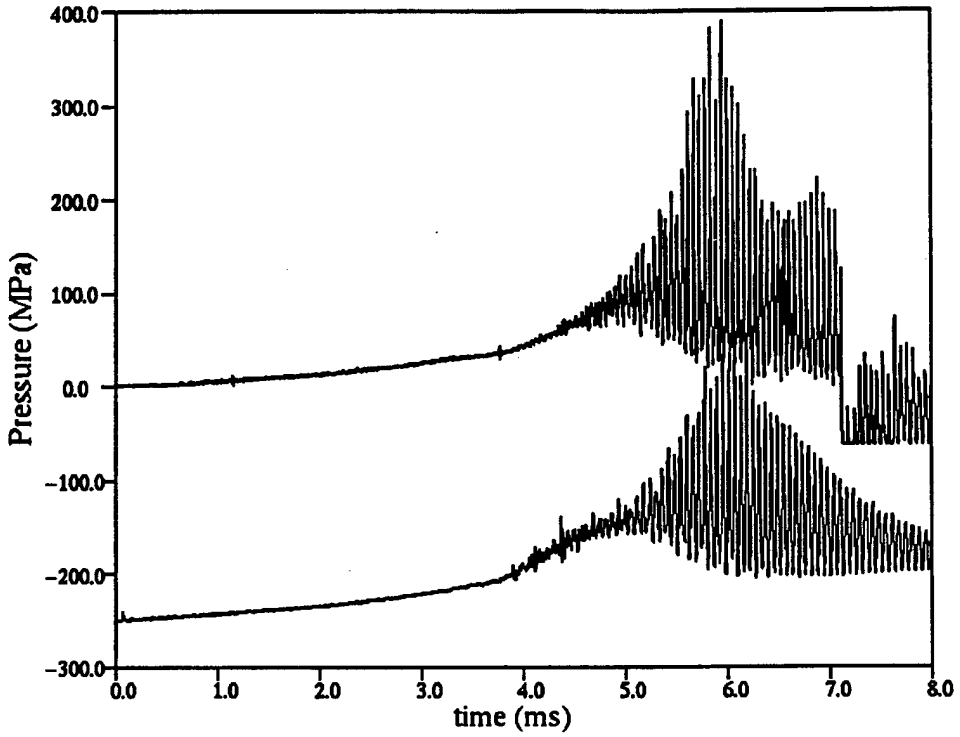

Figure 15. 30-mm Gun, Round 161. Control Piston Gauge (Top). Intact-Core Model, C = 3 (Bottom).

The Fourier transforms are shown in Figures 16–18. The code does generate about the correct frequency. The magnitude is much too low at the B plane. However, it is about correct at the A plane, and at the center line. These model parameters were the first time that the code generated a large oscillation near 19 kHz at the center line.

Analysis of the model shows some combustion on top of the core. There is a substantial amount of combustion at the end of the core. There is also a great deal of combustion under the core, past the end of the control piston. This is what generates the first radial mode for the cylinder. If the core is made shorter, the strong 19-kHz signal is not generated.

If the liquid is assumed to instantaneously break up into small drops, pressure oscillations are not generated. There is no noticeable accumulation, and pressure waves cannot build up. However, in the present model the core holds the liquid accumulation. Small droplets appear all around the core, rather than just at the injector.

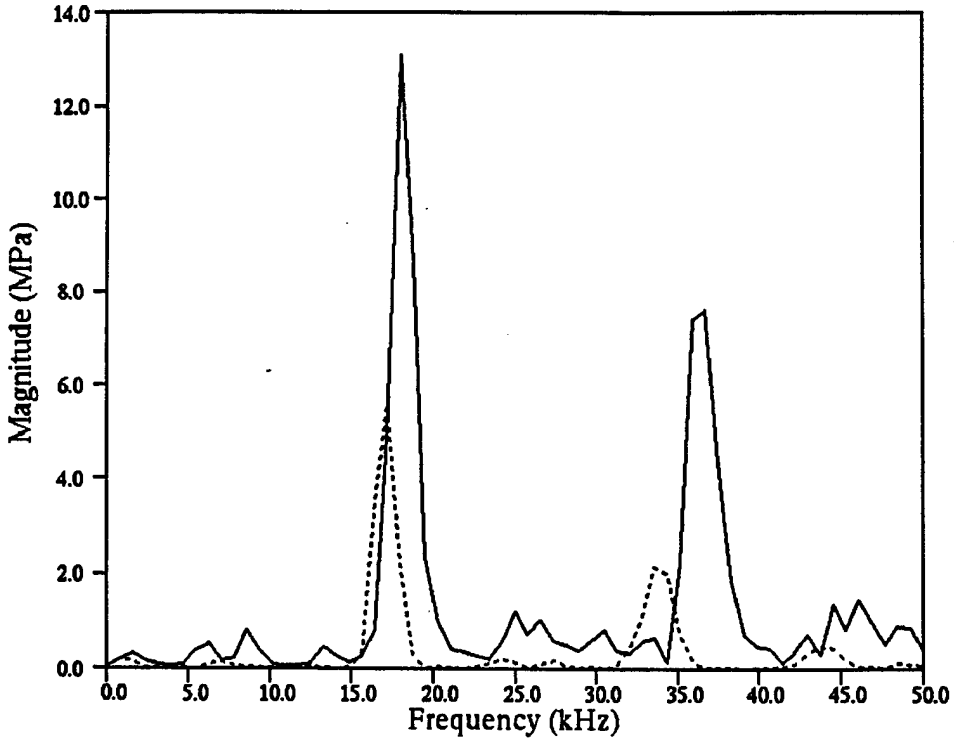

Figure 16. 30-mm Gun, Round 161. FFT, 5.5–6.5 ms. B30 Gauge (Line). Intact-Core Model, C = 3 (Dot).

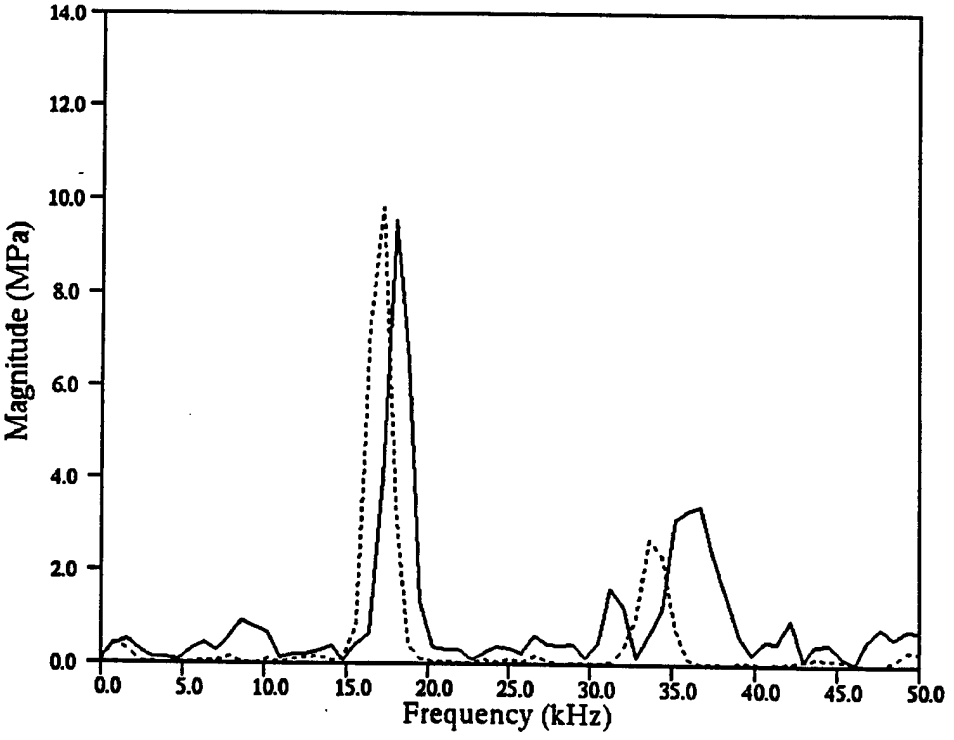

Figure 17. 30-mm Gun, Round 161. FFT, 5.5–6.5 ms. A90 Gauge (Line). Intact-Core Model, C = 3 (Dot).

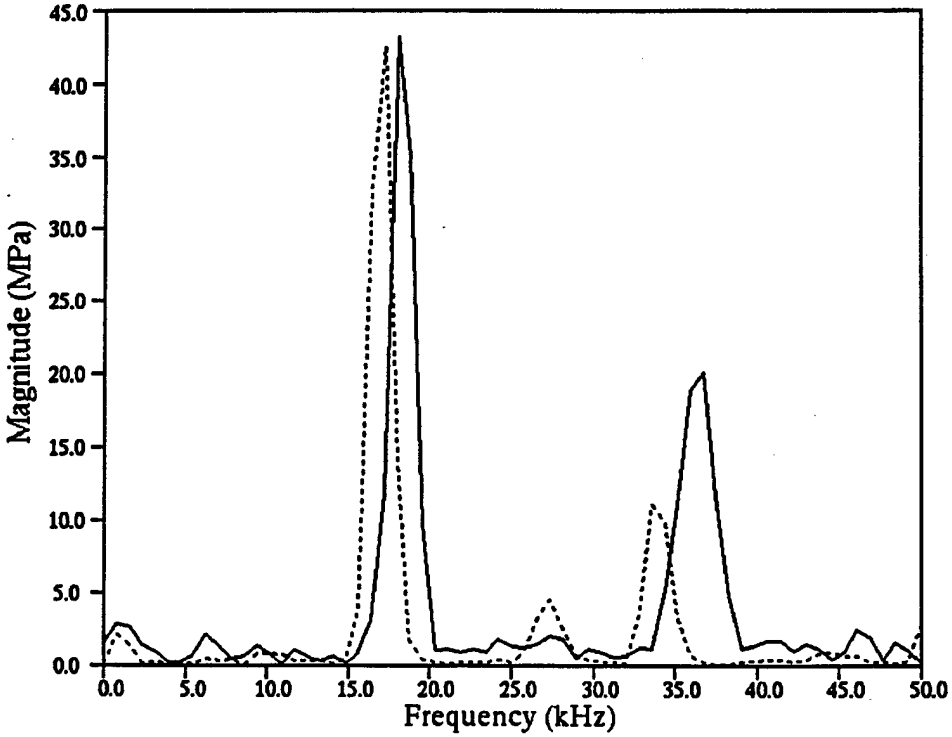

Figure 18. 30-mm Gun, Round 161. FFT, 5.5–6.5 ms. Control Piston Gauge (Line). Intact-Core Model, C = 3 (Dot).

The new model is much less sensitive to the burning rate. In fact, the aforementioned results were obtained with the lower strand-burner rate. If the closed-chamber rate is used instead, the oscillations are only slightly larger.

The model shows larger oscillations at the A plane, while the data show larger oscillations at the B plane. In the model, a longitudinal mode is set up at the top of the chamber, as well as the primary radial mode. This wave reinforces at the A plane and interferes at the B plane. A number of other parameters were tried in the model, without changing this fundamental pattern. The model is apparently too simplified to obtain the precise chamber behavior.

The current status of the code is that it generates a strong first-radial mode at the center line, and it gives good results using the more accurate combustion rate. The oscillations produced in the model are somewhat too small at the B plane.

8. Flow Dispersers

Impressive reductions in pressure oscillations have been obtained in the 30-mm RLPG using flow splitters or dispersers. The most effective designs have been nonaxisymmetric. The model was extended to 3-D partly to study flow dispersers. However, the model was not accurate, showing only a small effect on the pressure oscillations (Coffee 1995a). This disappointing result was part of the motivation for this report.

Baseline shots were fired before the shots with the flow dispersers. While the baseline conditions were very similar to round 161, discussed earlier, the results were a little different. Figures 19 and 20 show the Fourier transforms of the data at the B30 and A90 gauges. At the B plane, the strongest signal is 24 kHz (first radial for the annulus). At the A plane, the strongest

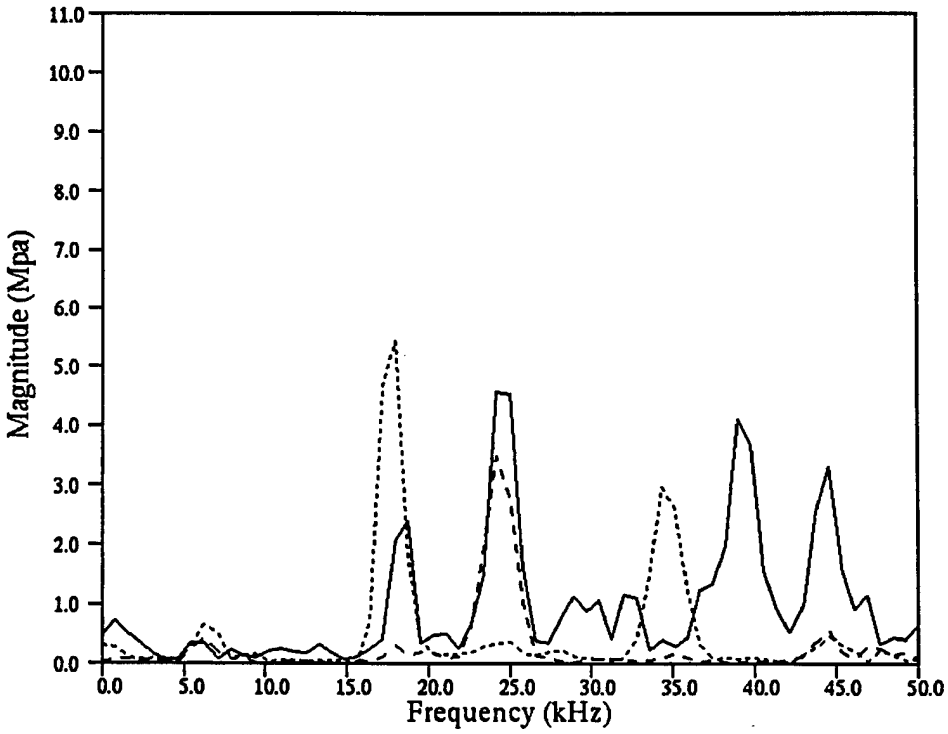

Figure 19. 30-mm Gun, Round 119. FFT, 5.5–6.5 ms. B30 Gauge (Line). Intact-Core Model, C = 3 (Dot). C = 1 (Dash).

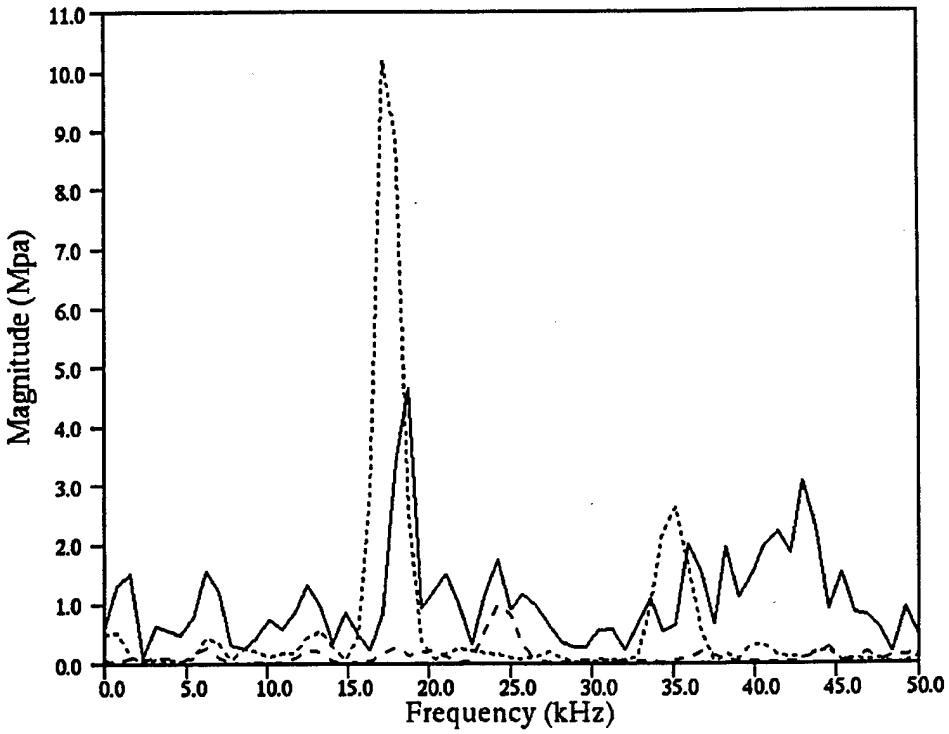

Figure 20. 30-mm Gun, Round 119. FFT, 5.5–6.5 ms. A90 Gauge (Line). Intact-Core Model, C = 3 (Dot). C = 1 (Dash).

signal is 19 kHz (first radial for the cylinder). The intact-core model was run with the multiplying constant C = 3 and C = 1. With the longer core, the results were similar to the previous case. The strongest signal was at 17 kHz, with the oscillations larger at the A plane than at the B plane. With the shorter core, the strongest signal was at 24 kHz, with the oscillations larger at the B plane than at the A plane. It proved impossible to generate both modes at once in the model. This is probably due to the simplification of the jet breakup and combustion processes.

A number of flow dispersers were tested in the 30-mm gun, including three axisymmetric concepts. While these splitters were less successful in reducing oscillations, they did have a major effect on the excited frequencies. These tests were completed before the through ports were put into the 30-mm gun.

A 45° conical disperser was modeled first as a 2-D calculation. The initial grid for the calculation is shown in Figure 21. The splitter was attached to the control piston with a hex bolt, which is approximated as a circular obstruction.

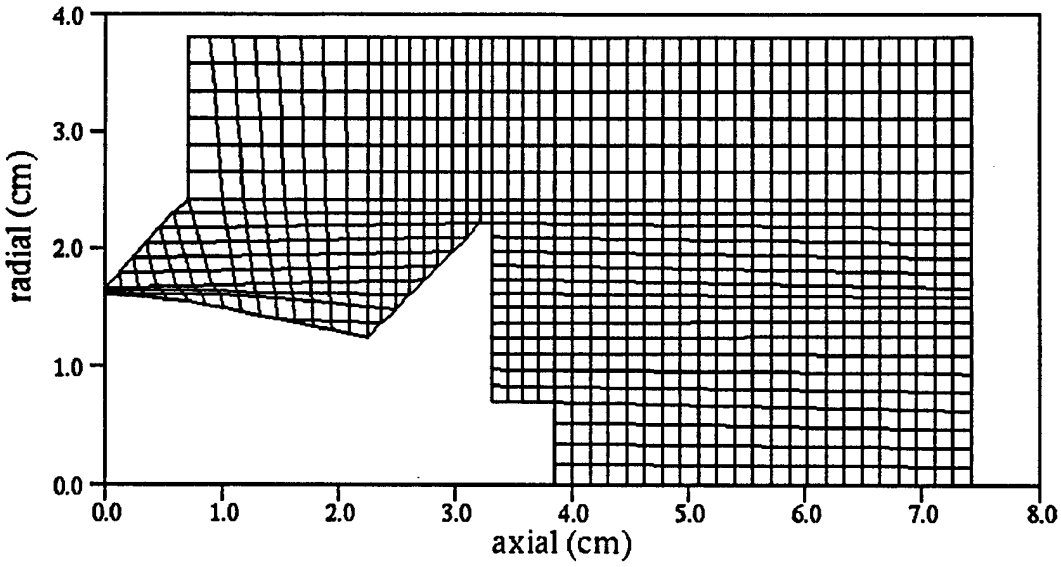

Figure 21. 30-mm Gun, Round 43. Axisymmetric 45° Conical Disperser. Initial 50 × 24 Grid.

In Figures 22 and 23, the Fourier transforms are shown. The disperser eliminates the usual 18-kHz and 23-kHz signals. However, new frequencies are excited. The most prominent is at 28 kHz. The large frequency near 50 kHz may be an artifact of the two-diameter port.

Using C = 3 in the intact-core model, the oscillations are basically nonexistent. With this value, the length of the core is greater than the distance from the injector to the disperser, so all of the combustion takes place above the core. With C = 2, the jet does end before the splitter. It is reasonable to assume that the splitter will affect the length of the core as it interacts with the jet and the surrounding gas flow. The model also eliminates the usual modes, and generates a new mode at 32 kHz.

This new mode is longitudinal, with pressure waves bouncing between the injector and the disperser. The difference in frequency compared to the data may be due to errors in computing the sound speed in the two-phase mixture, which is sensitive to the exact distribution of gas and liquid.

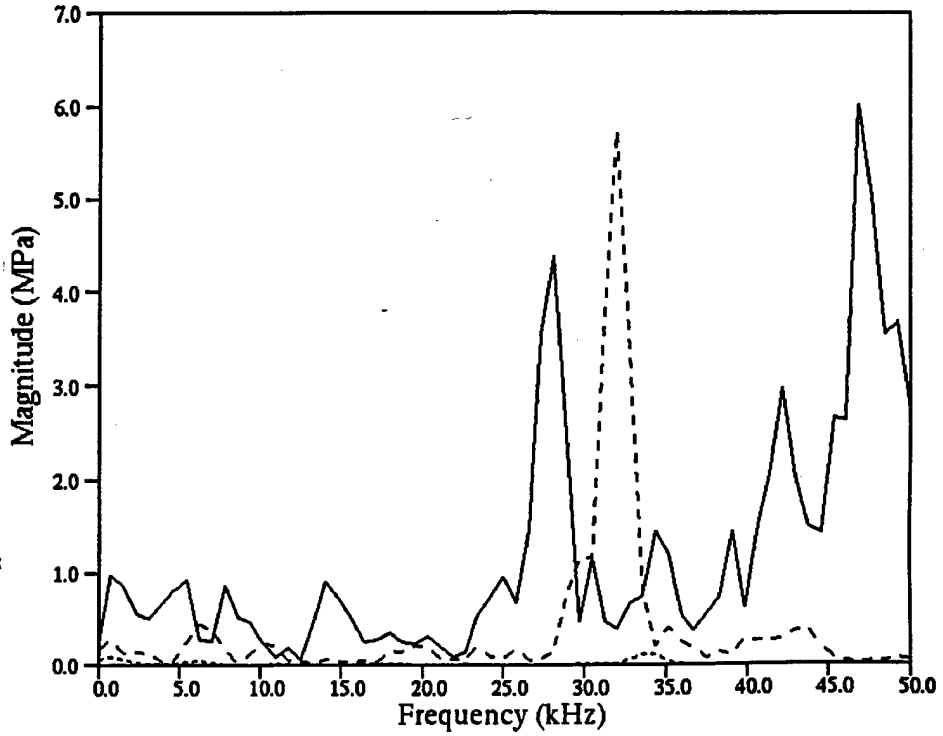

Figure 22. 30-mm Gun, Round 43. Axisymmetric Flow Disperser. FFT, 5.0–6.0 ms. B240 Gauge (Line). Intact-Core Model, C = 3 (Dot). C = 2 (Dash).

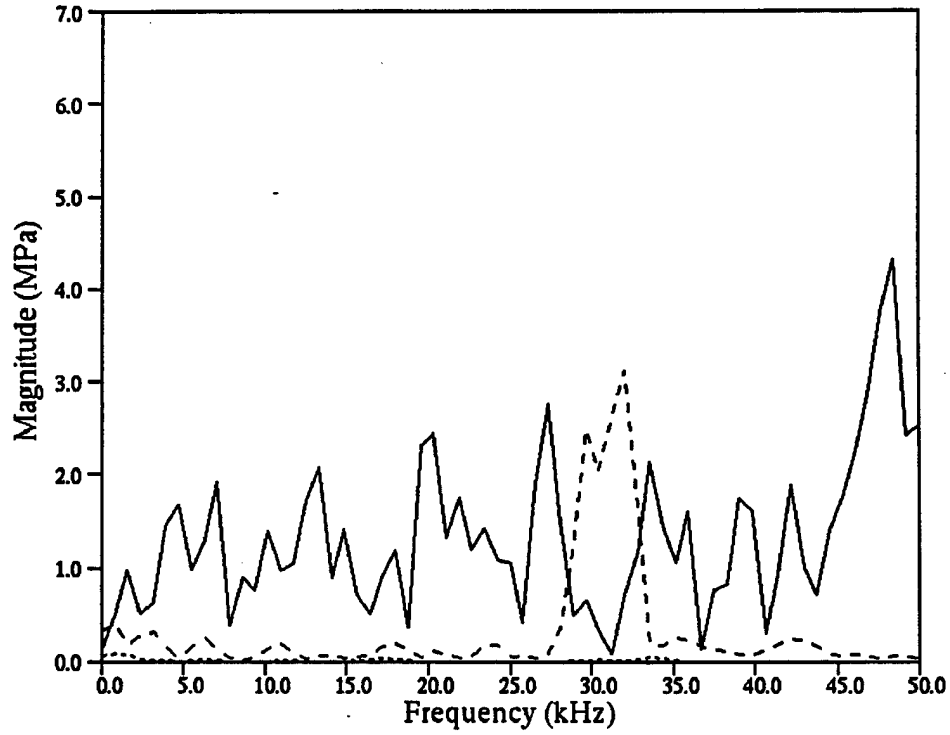

Figure 23. 30-mm Gun, Round 143. Axisymmetric Flow Disperser. FFT, 5.0–6.0 ms. A120 Gauge (Line). Intact-Core Model, C = 3 (Dot). C = 2 (Dash).

The previous droplet model gives similar results. As long as the combustion is between the injector and the splitter, the primary mode generated is longitudinal. This is the likely occurrence in the experiment.

The most effective flow disperser in the 30-mm gun was the 45° daisywheel. This splitter has eight three-sided blades designed to deflect the flow from the regenerative injector region. The model takes advantage of the symmetry and only represents one of the blades. Figure 24 shows part of the initial 50 × 24 × 22 grid. The orientation of the disperser in the gun was not recorded, so, arbitrarily, the low point between blades is located at 0°. The simulation required about a week of CPU time on a Silicon Graphics Power Challenge Array.

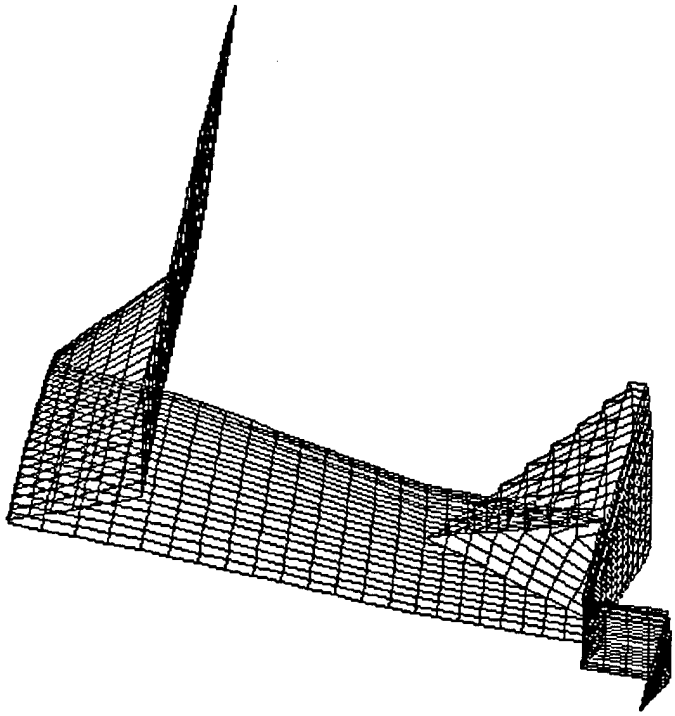

Figure 24. 30-mm Gun, 45° Daisywheel Disperser, Round 122. Initial 50 × 24 × 22 Grid.

The intact-core model was run with C = 3. The Fourier transforms are shown in Figures 25 and 26. The model now accurately simulates the drastic reduction in the magnitude of the oscillations.

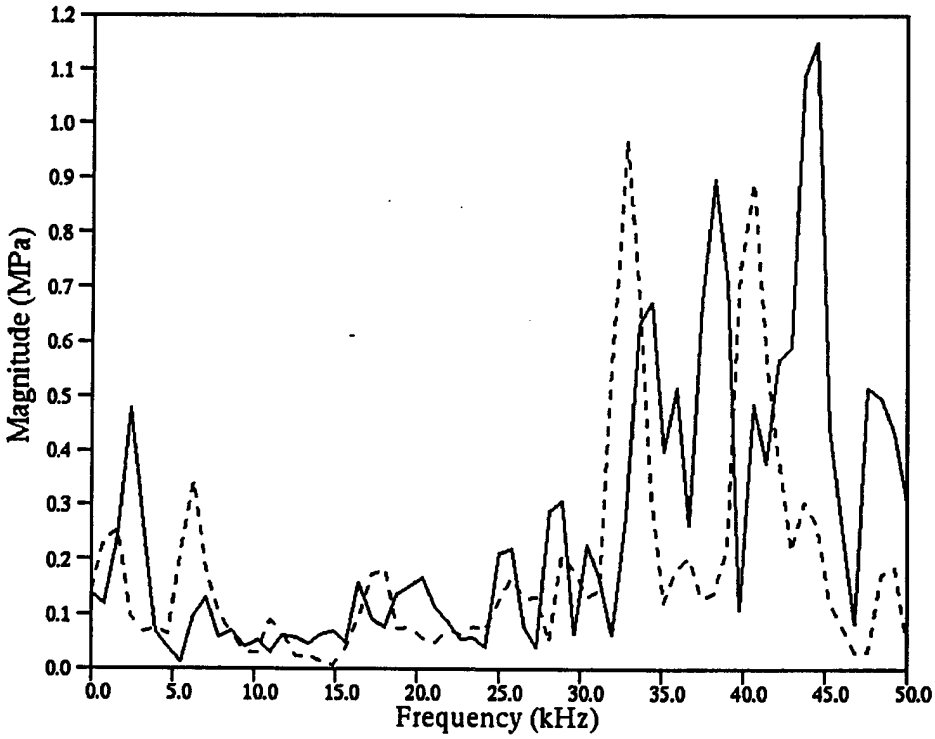

Figure 25. 30-mm Gun, 45° Daisywheel Disperser, Round 122. FFT, 5.5–6.5 ms. B30 Gauge (Line). Intact-Core Model, C = 3 (Dash).

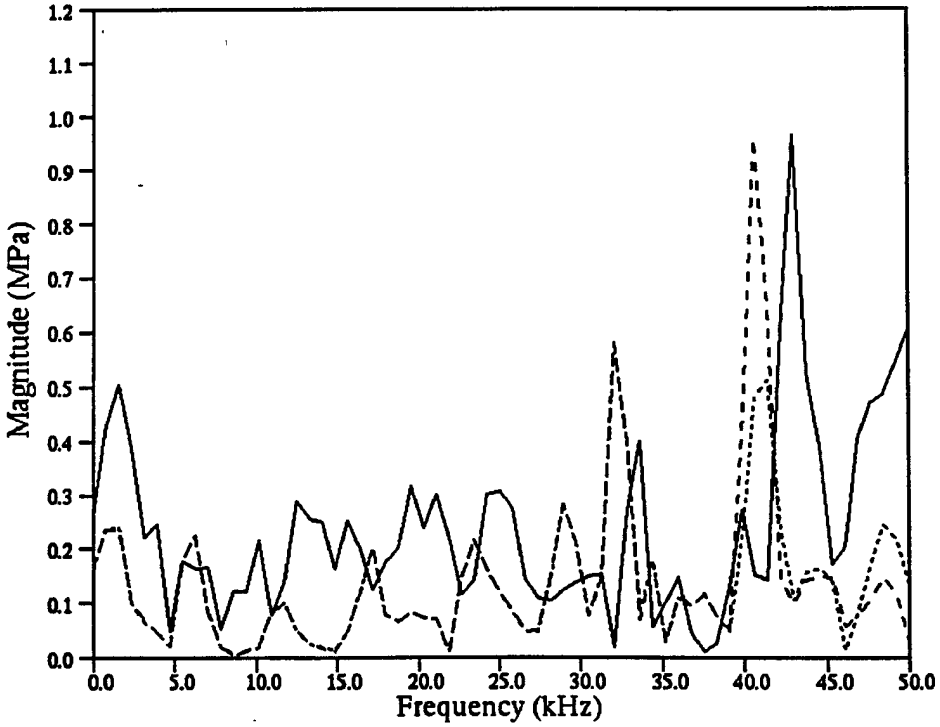

Figure 26. 30-mm Gun, 45° Daisywheel Disperser, Round 122. FFT, 5.5–6.5 ms. A90 Gauge (Line). Intact-Core Model, C = 3. A30 (Dot). A90 (Dash).

In the data, the largest remaining frequency was at 43 kHz. The model comes close to this with a relatively large 41-kHz frequency. Animation of the simulation results reveals an apparent 3-D mode, with pressure waves bouncing at an angle between the blades of the disperser and the injection piston. Much of the combustion takes place between the blades of the piston. The 41-kHz signal is stronger at some locations than at others (see Figure 26). Since the orientation of the disperser in the gun is not known, the tangential pattern in the model cannot be compared with the data.

Runs were made with a longer control piston, without disperser blades. A smaller reduction in the pressure oscillations was observed compared to the baseline. Some of the reduction in pressure oscillations may be because hot gas can no longer get under the core at the end of the control piston.

9. 155-mm Guns

Flow dispersers were also incorporated in the 155-mm gun number two. The dispersers did not extend as far up radially as in the 30-mm gun. A 45° daisywheel disperser worked well for a 4-liter charge. Unfortunately, the simulation indicated that the flow disperser has very little effect on the oscillations. Most of the combustion takes place above the disperser. It is possible that the model does not resolve the motion of the core properly, and that the combustion does take place closer to the splitter.

For a 7.1-liter charge, the splitter in the experiment had very little effect. However, a modified splitter that was set another 1.2 cm back from the injector proved effective. This suggests a critical distance for a splitter to work effectively. It is postulated that if the disperser is too close to the injector, the core combusts past the disperser, still generating large oscillations. Further research is needed on 155-mm guns.

10. Conclusions

Additional physics submodels have been added to the 2-D/3-D code LPOSC, to describe independent piston motion, drag between the liquid and gas phases, droplet distribution, heat transfer to the liquid, and ignition delay. The new version of the code runs about 10 times slower than the old version. While increasing the accuracy of the comparison between experiment and simulation in some cases, the overall ability of the model to explain experimental results was not substantially increased.

Based on these results, an intact-core model was developed. With this model, the baseline 30-mm firings, the shots with pressure measured on the control piston, and the flow disperser shots were accurately modeled. Moreover, the more accurate strand-burner combustion rate was used instead of the closed-chamber rate used previously. Unfortunately, the new model is not as accurate for 155-mm-gun firings, and work on these cases is proceeding.

Based on the modeling, the following conclusions can be made. Most of the injected liquid is in the intact core or in a very dense noncombusting spray. When the liquid breaks up, it rapidly forms small droplets that quickly ignite and burn. The simulations still show a simpler frequency structure than the data. To make the problem tractable, the jet breakup and combustion must be simplified, and the grid must be relatively coarse.

The model suggests that flow dispersers in the 30-mm gun reduce oscillations not by physically dispersing the jet, but by locating the combustion between the blades of the jet. This implies that if a disperser is to be effective for a range of charge sizes, the blades must be made longer. However, this conclusion is only tentative, and further research on jet breakup and data from the 155-mm gun are needed.

INTENTIONALLY LEFT BLANK.

11. References

Birk, A., M. McQuaid, and M. Gross. "Liquid Core Structure of Evaporating Sprays at High Pressures - Flash X-Ray Studies." ARL-TR-901, U.S. Army Research Laboratory, Aberdeen Proving Ground, MD, December 1995.

Coffee, T. P. "A Lumped Parameter Code for Regenerative Liquid Propellant Guns." BRL-TR-2703, U.S. Army Ballistic Research Laboratory, Aberdeen Proving Ground, MD, December 1985.

Coffee, T. P. "An Updated Lumped Parameter Code for Regenerative Liquid Propellant In-Line Guns." BRL-TR-2974, U.S. Army Ballistic Research Laboratory, Aberdeen Proving Ground, MD, December 1988.

Coffee, T. P. "A Two-Dimensional Model for the Combustion Chamber/ Gun Tube of a Concept VIC Regenerative Liquid Propellant Gun." BRL-TR-3341, U.S. Army Ballistic Research Laboratory, Aberdeen Proving Ground, MD, May 1992.

Coffee, T. P. "A Two-Dimensional Model for Pressure Oscillations: Extension to Generalized Geometry." ARL-TR-349, U.S. Army Research Laboratory, Aberdeen Proving Ground, MD, January 1994.

Coffee, T. P. "Modeling of Flow Splitters in Regenerative Liquid Propellant Guns." CPIA Publication no. 631, vol. III, pp. 257–268, October 1995a.

Coffee, T. P. "A Three-Dimensional (3-D) Model for Pressure Oscillations in a Regenerative Liquid Propellant Gun (RLPG)." ARL-TR-897, U.S. Army Research Laboratory, Aberdeen Proving Ground, MD, November 1995b.

Coffee, T. P., P. G. Baer, W. F. Morrison, and G. P. Wren. "Jet Breakup and Combustion Modeling for the Regenerative Liquid Propellant Gun." BRL-TR-3223, U.S. Army Ballistic Research Laboratory, Aberdeen Proving Ground, MD, April 1991.

Coffee, T. P., and G. P. Wren. "Analysis of Repeatability Data for the Second-Generation 155-mm Concept VIC Regenerative Liquid Propellant Gun (RLPG)." ARL-TR-1157, U.S. Army Research Laboratory, Aberdeen Proving Ground, MD, July 1996.

Colburn, J., T. Coffee, A. Johnson, M. Ridgley, G. Sprenkle, T. Rosenberger, and J. Knapton. "Measurement of Pressure on the Face of the Control Piston in a 30-mm Concept VIC Regenerative Liquid Propellant Gun." CPIA Publication no. 631, vol. III, pp. 313–322, October 1995.

Faeth G. M., L. P. Hsiang, and P. K. Wu. "Structure and Breakup Properties of Sprays." *International Journal of Multiphase Flow*, vol. 21, pp. 99–127, 1995.

Fox, R. W., and A. T. McDonald. *Introduction to Fluid Mechanics*. John Wiley and Sons, 1985.

Gough, P. S. "A Two-Phase Model of the Interior Ballistics of Hybrid Solid-Propellant Traveling Charges." PGA-TR-83-3, September 1983.

Klein, N. Private communication. U.S. Army Ballistic Research Laboratory, Aberdeen Proving Ground, MD, 1992.

Klein, N., C. S. Leveritt, and P. G. Baer. "The Effects of Composition Variation and Nitric Acid on the Stability and Reactivity of the HAN-Based Liquid Propellants." BRL-TR-3179, U.S. Army Ballistic Research Laboratory, Aberdeen Proving Ground, MD, January 1991.

McBratney, W. F. "Windowed Chamber Investigation of the Burning Rate of Liquid Monopropellant for Guns." BRL-MR-03018, U.S. Army Ballistic Research Laboratory, Aberdeen Proving Ground, MD, April 1980.

McBratney, W. F. "Burning Rate Data, LPG1845." BRL-MR-03128, U.S. Army Ballistic Research Laboratory, Aberdeen Proving Ground, MD, August 1981.

McBratney, W. F., and J. A. Vanderhoff. "High Pressure Windowed Chamber Burn Rate Determination of Liquid Propellant XM46." ARL-TR-422, U.S. Army Research Laboratory, Aberdeen Proving Ground, MD, June 1994.

Oberle, W., and G. Wren. "Burn Rates of LPG1846 Conditioned Ambient, Hot, and Cold." BRL-TR-3287, U.S. Army Ballistic Research Laboratory, Aberdeen Proving Ground, MD, October 1991.

Ranz, W. E., and W. R. Marshall. "Evaporation From Drops." *Chemical Engineering Progress*, vol. 48, pp. 141–173, 1952.

Rosenberger, T. E. "Workshop Report: Measurement Techniques in Highly Transient, Spectrally Rich Combustion Environments." ARL-SR-18, U.S. Army Research Laboratory, Aberdeen Proving Ground, MD, September 1994.

Simmons, H. C. "The Correlation of Drop-Size Distributions in Fuel Nozzle Sprays." *Journal of Engineering Power*, vol. 99, pp. 309–319, 1977.

Wolfe, H. E., and W. H. Andersen. "Kinetics, Mechanism, and Resultant Droplet Sizes of the Aerodynamic Breakup of Liquid Drops." Aerojet Report No. 0395-04(18)SP, April 1964.

NO. OF
COPIES ORGANIZATION

2 DEFENSE TECHNICAL
INFORMATION CENTER
DTIC DDA
8725 JOHN J KINGMAN RD
STE 0944
FT BELVOIR VA 22060-6218

1 HQDA
DAMO FDQ
DENNIS SCHMIDT
400 ARMY PENTAGON
WASHINGTON DC 20310-0460

1 CECOM
SP & TRRSTRL COMMCTN DIV
AMSEL RD ST MC M
H SOICHER
FT MONMOUTH NJ 07703-5203

1 PRIN DPTY FOR TCHNLGY HQ
US ARMY MATCOM
AMCDCG T
M FISETTE
5001 EISENHOWER AVE
ALEXANDRIA VA 22333-0001

1 PRIN DPTY FOR ACQUSTN HQS
US ARMY MATCOM
AMCDCG A
D ADAMS
5001 EISENHOWER AVE
ALEXANDRIA VA 22333-0001

1 DPTY CG FOR RDE HQS
US ARMY MATCOM
AMCRD
BG BEAUCHAMP
5001 EISENHOWER AVE
ALEXANDRIA VA 22333-0001

1 DPTY ASSIST SCY FOR R&T
SARD TT T KILLION
THE PENTAGON
WASHINGTON DC 20310-0103

1 OSD
OUSD(A&T)/ODDDR&E(R)
J LUPO
THE PENTAGON
WASHINGTON DC 20301-7100

NO. OF
COPIES ORGANIZATION

1 INST FOR ADVNCD TCHNLGY
THE UNIV OF TEXAS AT AUSTIN
PO BOX 202797
AUSTIN TX 78720-2797

1 USAASA
MOAS AI W PARRON
9325 GUNSTON RD STE N319
FT BELVOIR VA 22060-5582

1 CECOM
PM GPS COL S YOUNG
FT MONMOUTH NJ 07703

1 GPS JOINT PROG OFC DIR
COL J CLAY
2435 VELA WAY STE 1613
LOS ANGELES AFB CA 90245-5500

1 ELECTRONIC SYS DIV DIR
CECOM RDEC
J NIEMELA
FT MONMOUTH NJ 07703

3 DARPA
L STOTTS
J PENNELLA
B KASPAR
3701 N FAIRFAX DR
ARLINGTON VA 22203-1714

1 USAF SMC/CED
DMA/JPO
M ISON
2435 VELA WAY STE 1613
LOS ANGELES AFB CA
90245-5500

1 US MILITARY ACADEMY
MATH SCI CTR OF EXCELLENCE
DEPT OF MATHEMATICAL SCI
MDN A MAJ DON ENGEN
THAYER HALL
WEST POINT NY 10996-1786

1 DIRECTOR
US ARMY RESEARCH LAB
AMSRL CS AL TP
2800 POWDER MILL RD
ADELPHI MD 20783-1145

NO. OF
COPIES ORGANIZATION

1 DIRECTOR
US ARMY RESEARCH LAB
AMSRL CS AL TA
2800 POWDER MILL RD
ADELPHI MD 20783-1145

3 DIRECTOR
US ARMY RESEARCH LAB
AMSRL CI LL
2800 POWDER MILL RD
ADELPHI MD 20783-1145

ABERDEEN PROVING GROUND

4 DIR USARL
AMSRL CI LP (305)

NO. OF COPIES ORGANIZATION

1 CDR USA ARDEC
AMSTA AR AEE B D DOWNS
PICATINNY ARSENAL NJ
07806-5000

3 CDR USA ARDEC
AMSTA AR FSS DA R KOPMANN
B MACHEK
J IRIZARRY
PICATINNY ARSENAL NJ
07806-5000

1 DIR
BENET WPNS LAB
AMSTA AR CCB RA G P OHARA
WATERVLIET NY 12189-4050

2 CDR ARO
TECH LIBRARY
D MANN
PO BOX 12211
RESEARCH TRIANGLE PARK NC
27709-2211

1 CMDT
USA CGSC
FT LEAVENWORTH KS 66027

2 DIR DARPA
J LUPO
J RICHARDSON
1400 WILSON BVLD
ARLINGTON VA 22209

1 CDR NASC
AIR 954 TECH LIBRARY
WASHINGTON DC 20360

1 SPRNTNDNT
NAVAL PSTGRDT SCHL
DEPT OF MECH ENGNRNG
CODE 1424 LIBRARY
MONTEREY CA 93943

4 CDR NRL
TECH LIBRARY
CODE 4410 K KAILASANATE
J BORIS
E ORAN
WASHINGTON DC 20375-5000

NO. OF COPIES ORGANIZATION

1 OFFICE OF NAVAL RSCH
CODE 473 R S MILLER
800 NORTH QUINCY ST
ARLINGTON VA 22217-9999

1 CDR NAWC
INFORMATION SCIENCE DIVISION
CHINA LAKE CA 93555-6001

3 CDR NSWC
CODE E23 TECH LIBRARY
CODE G30 GUNS & MNTNS DIV
CODE G32 GUNS SYS DIV
DAHLGREN VA 22448-5000

1 CDR NUSC
CODE 5B331 TECH LIBRARY
NEWPORT RI 02840

3 AL LSCF
J LEVINE
L QUINN
T EDWARDS
EDWARDS AFB CA 93523-5000

2 DIR NASA
MS 603 TECH LIBRARY
MS 86 DR POVINELLI
21000 BROOKPARK RD
LEWIS RSCH CTR
CLEVELAND OH 44135

2 NASA LANGLEY RSCH CTR
MS 408 W CALLION
D WITCOFSKI
HAMPTON VA 23605

1 DIR JET PRPLSN LAB
TECH LIBRARY
4800 OAK GROVE DR
PASADENA CA 91109

2 DIR LLNL
1355 A BUCKINGHAM
M FINGER
PO BOX 808
LIVERMORE CA 94550-0622

NO. OF
COPIES ORGANIZATION

1 DIR LOS ALAMOS SCNTFC LAB
T3 D BUTLER
PO BOX 1663
LOS ALAMOS NM 87544

1 DIR SNL
R CARLING CMBSTN RSCH FAC
LIVERMORE CA 94551-0469

1 INST FOR DFNS ANLYS
D SPARROW
1801 NO BEAUREGARD ST
ALEXANDRIA VA 22311-1772

1 PA STATE UNIV
DEPT OF MCHNCL ENGNRNG
K K KUO
140 RSRCH BLDG EAST
UNIVERSITY PARK PA 16802

1 PA STATE UNIV
DEPT OF MCHNCL ENGNRNG
S T THYNELL
309 REBER BLDG
UNIVERSITY PARK PA 16802

1 UNIV OF MN
ARMY HPC RSCH CTR
T E TEZDUYAR
1100 WASHINGTON AVE SO STE 101
MINNEAPOLIS MN 55415

3 CMBSTN RSCH AND FLOW TECH INC
S DASH
A HOSANGADI
N SINHA
174 NO MAIN ST BLDG 3
PO BOX 1150
DUBLIN PA 18917

1 GEN DYNMCS DFNS SYS
PCRL DIV N A MESSINA
PRINCETON CORP PLZ
11 DEERPRK DR BLDG IV STE 119
MONMOUTH JUNCTION NJ 08852

NO. OF
COPIES ORGANIZATION

6 GEN DYNMCS DFNS SYS
C BANKER
B FEATHEROFF
G KEELER
M TWEED KENT
T KURIATA
I MAGOON
100 PLASTICS AVE
PITTSFIELD MA 01201-3698

1 PAUL GOUGH ASSOCIATES
P S GOUGH
1048 SOUTH ST
PORTSMOUTH NH 03801-5423

1 PHYSICS INTRNTNL LIBRARY
H WAYNE WAMPLER
PO BOX 5010
SAN LEANDRO CA 94577-0599

1 SRI INTERNATIONL
TECH LIBRARY
PROPULSION SCIENCES DIV
333 RAVENWOOD AVE
MENLO PARK CA 94025-3493

1 VERITAY TECH INC
E FISHER
4845 MILLERSPORT HWY
EAST AMHERST NY 14501-0305

ABERDEEN PROVING GROUND

2 DIR AMSAA
AMXSY-D
AMXSY-MP, H. COHEN

1 CDR, TECOM
AMSTE-TO-F

3 CDR, CRDEC, AMCCOM
SMCCR-RSP-A
SMCCR-MU
SMCCR-SPS-IL

NO. OF
COPIES ORGANIZATION

ABERDEEN PROVING GROUND

30 DIR, USARL
AMSRL-WM-P, A. HORST
AMSRL-WM-PA,
A. BIRK
L-M CHANG
T. COFFEE (5 CP)
J. COLBURN
P. CONROY
J. DESPIRITO
A. JUHASZ
G. KELLER
J. KNAPTON
D. KOOKER
C. LEVERITT
T. MINOR
M. NUSCA
W. OBERLE
S. RAY
T. ROSENBERGER
K. WHITE
G. WREN (5 CP)
AMSRL-WM-PB, P. PLOSTINS
AMSRL-WM-PC, B. FORCH
AMSRL-WM-PD, B. BURNS

NO. OF
COPIES ORGANIZATION

1 MR CLIVE WOODLEY
GS2 DIV BLDG R31
RARDE-FT HALSTEAD
SEVENOAKS KENT TN14 7BT
ENGLAND

1 DFNC SCNC AND TECH ORGNZTN
ANNA WILDEGGER-GAISSMAJER
PO BOX 1500
SALISBURY SO AUSTRALIA 5108
AUSTRALIA

REPORT DOCUMENTATION PAGE

Form Approved
OMB No. 0704-0188

1. AGENCY USE ONLY *(Leave blank)*	2. REPORT DATE	3. REPORT TYPE AND DATES COVERED
	January 1998	Final, Jan 95 - Apr 97

4. TITLE AND SUBTITLE
Progress in Modeling Pressure Oscillations in 30-mm Regenerative Liquid Propellant Guns (RLPGs)

5. FUNDING NUMBERS
PR: 1L16261841FL

6. AUTHOR(S)
Terence P. Coffee

7. PERFORMING ORGANIZATION NAME(S) AND ADDRESS(ES)
U.S. Army Research Laboratory
ATTN: AMSRL-WM-PA
Aberdeen Proving Ground, MD 21005-5066

8. PERFORMING ORGANIZATION REPORT NUMBER
ARL-TR-1582

9. SPONSORING/MONITORING AGENCY NAMES(S) AND ADDRESS(ES)

10.SPONSORING/MONITORING AGENCY REPORT NUMBER

11. SUPPLEMENTARY NOTES

12a. DISTRIBUTION/AVAILABILITY STATEMENT
Approved for public release; distribution unlimited.

12b. DISTRIBUTION CODE

13. ABSTRACT *(Maximum 200 words)*

Regenerative liquid propellant guns (RLPG) have been studied for many years. RLPG gun firings almost always show large high-frequency pressure oscillations. To study this phenomenon, a two-dimensional (2-D) axisymmetric fluid dynamics model of the combustion chamber/gun tube of an RLPG has been developed. High-frequency oscillations are generated naturally by the code. Recently, the code has been extended to three dimensions (3-D).

The results generally compare well with RLPG data; however, there are some recent cases that the code does not represent well. In this report, several extensions to the program are discussed in an attempt to improve the fidelity of the code. The most useful extension has been an intact-core model.

14. SUBJECT TERMS	15. NUMBER OF PAGES
fluid dynamics, liquid gun propellants, regenerative gun, pressure oscillations, two- dimensional model, three-dimensional model	48
	16. PRICE CODE

17. SECURITY CLASSIFICATION OF REPORT	18. SECURITY CLASSIFICATION OF THIS PAGE	19. SECURITY CLASSIFICATION OF ABSTRACT	20. LIMITATION OF ABSTRACT
UNCLASSIFIED	UNCLASSIFIED	UNCLASSIFIED	UL

INTENTIONALLY LEFT BLANK

USER EVALUATION SHEET/CHANGE OF ADDRESS

This Laboratory undertakes a continuing effort to improve the quality of the reports it publishes. Your comments/answers to the items/questions below will aid us in our efforts.

1. ARL Report Number/Author ARL-TR-1582 (Coffee) Date of Report January 1998

2. Date Report Received _____

3. Does this report satisfy a need? (Comment on purpose, related project, or other area of interest for which the report will be used.) _____

4. Specifically, how is the report being used? (Information source, design data, procedure, source of ideas, etc.) _____

5. Has the information in this report led to any quantitative savings as far as man-hours or dollars saved, operating costs avoided, or efficiencies achieved, etc? If so, please elaborate. _____

6. General Comments. What do you think should be changed to improve future reports? (Indicate changes to organization, technical content, format, etc.) _____

CURRENT ADDRESS

Organization

Name E-mail Name

Street or P.O. Box No.

City, State, Zip Code

7. If indicating a Change of Address or Address Correction, please provide the Current or Correct address above and the Old or Incorrect address below.

OLD ADDRESS

Organization

Name

Street or P.O. Box No.

City, State, Zip Code

(Remove this sheet, fold as indicated, tape closed, and mail.)

(DO NOT STAPLE)

DEPARTMENT OF THE ARMY

OFFICIAL BUSINESS

NO POSTAGE
NECESSARY
IF MAILED
IN THE
UNITED STATES

BUSINESS REPLY MAIL
FIRST CLASS PERMIT NO 0001,APG,MD

POSTAGE WILL BE PAID BY ADDRESSEE

DIRECTOR
US ARMY RESEARCH LABORATORY
ATTN AMSRL WM PA
ABERDEEN PROVING GROUND MD 21005-5066